From Department of Molecular Medicine and Surgery (MMK)
Karolinska Institutet, Stockholm, Sweden

ELECTROCARDIOGRAPHIC CHARACTERIZATION OF MYOCARDIAL SCAR IN PRESENCE OF CONDUCTION ABNORMALITY

Björn Wieslander

Karolinska Institutet

Stockholm 2016

Cover:

Superimposed 12-lead ECG from a patient with
left bundle branch block. Hidden beneath
the transparent electrocardiographic signal
is a late gadolinium enhancement
cardiovascular magnetic resonance image
with evidence of previous myocardial infarction.

All previously published papers were reproduced with permission from the publisher.
Published by Karolinska Institutet.
Printed by Eprint AB 2016
© Björn Wieslander, 2016
ISBN 978-91-7676-420-6

Electrocardiographic characterization of myocardial scar in presence of conduction abnormality

THESIS FOR DOCTORAL DEGREE (Ph.D.)

Publicly defended in Lilla Salen, Q3, Astrid Lindgren Children's Hospital, Karolinska University Hospital

Friday November 4th 2016 at 9:00 A.M.

By

Björn Wieslander

Principal Supervisor:
Martin Ugander, MD, PhD
Karolinska Institutet
Department of Molecular Medicine and Surgery
Division of Clinical Physiology

Co-supervisors:
David G. Strauss, MD, PhD
Karolinska Institutet
Department of Molecular Medicine and Surgery
Division of Clinical Physiology

Andreas Sigfridsson, PhD
Karolinska Institutet
Department of Molecular Medicine and Surgery
Division of Clinical Physiology

Kenneth Caidahl, MD, PhD
Karolinska Institutet
Department of Molecular Medicine and Surgery
Division of Clinical Physiology

Opponent:
Olujimi Ajijola, MD, PhD
University of California Los Angeles
Cardiac Arrhythmia Center and Neurocardiology
Research Center of Excellence

Examination Board:
Erik Hedström, MD, PhD
Lund Universitet
Department of Clinical Sciences

Frieder Braunschweig, MD, PhD
Karolinska Institutet
Department of Medicine

Sverker Jern, MD, PhD
Göteborgs Universitet
Department of Molecular and Clinical Medicine

“The chains of habit are too weak to be felt

until they are too heavy to be broken”

Samuel Johnson

ABSTRACT

Presence, extent and localization of myocardial scar constitute prognostic clinical information that can influence therapeutical decisions. Cardiovascular magnetic resonance imaging with late gadolinium enhancement (CMR-LGE) is the preferred method to image myocardial scar *in vivo* but is resource intensive and has contraindications. The 12-lead electrocardiogram (ECG) is less accurate but inexpensive and widely available. Adaptations of the Selvester QRS score, an ECG analysis system for scar characterization, were developed in 2009 for use in presence of conduction abnormalities such as left bundle branch block (LBBB). Prior to the work described in this thesis, these newly developed Selvester QRS score adaptations had only been preliminarily validated against CMR-LGE.

The overall aim of the thesis was to evaluate the diagnostic performance and clinical utility in predicting response to cardiac resynchronization therapy (CRT) of the 2009 Selvester QRS score for use in the presence of conduction abnormality, and to revise the LBBB version (2009 LBSS) based on empirical CMR-LGE data.

We found that the ECG criteria comprising the 2009 LBSS had modest ability to localize CMR-LGE verified myocardial scar within the left ventricle (LV) (study I). Next, we evaluated the ability of the Selvester QRS score adaptations for use in LBBB, right bundle branch block (RBBB), left anterior fascicular block (LAFB) and combined RBBB+LAFB to identify and quantify myocardial scar as verified by CMR-LGE. The results revealed a tendency of the ECG method to overestimate scar burden and presence compared to CMR-LGE (study II). We then investigated the individual specificity of the 46 QRS morphology criteria that comprise the 2009 LBSS and found that certain criteria hade prohibitively low specificity, likely causing the overestimation of myocardial scar size and presence found previously (study III). We further evaluated the ability of all Selvester QRS score adaptations to predict response to CRT in a randomized cohort. Scar burden estimated by QRS scoring did predict clinical outcome in both study arms but could not distinguish who benefitted from CRT in terms of reduced risk of heart failure event or death (study IV). Finally, we assembled a large training dataset of 325 patients in which we performed careful continuous measurements on digital ECGs. We subsequently compared ECG measurements to myocardial scar quantified by CMR-LGE. We achieved an improved method of ECG scar detection in LBBB compared to the 2009 LBSS that remains to be tested in an independent population.

The Selvester QRS score adaptations for presence of conduction abnormalities tends to overestimate scar and has limited correlation with CMR-LGE verified scar presence and extent. The 12-lead ECG likely contains insufficient information for accurate quantification of myocardial scar in LBBB. However, it may still be possible to distinguish between scar presence and absence using the 12-lead ECG in presence of LBBB.

LIST OF STUDIES

I. **Wieslander B**, Wu KC, Loring Z, Andersson LG, Frank TF, Gerstenblith G, Tomaselli GF, Weiss RG, Wagner GS, Ugander M and Strauss DG. Localization of myocardial scar in patients with cardiomyopathy and left bundle branch block using electrocardiographic Selvester QRS scoring. *J Electrocardiol*. 2013;26:00049-6.

II. **Wieslander B**, Nijveldt R, Klem I, Lokhnygina Y, Pura J, Wagner GS, Ugander M and Atwater BD. Evaluation of Selvester QRS score for use in presence of conduction abnormalities in a broad population. *Am Heart J*. 2015;170:346-52.

III. Åkerlund S, **Wieslander B**, Turesson M, Nijveldt R, Klem I, Almer J, Engblom H, Wagner GS, Atwater BD and Ugander M. Specificity for each of the 46 criteria of the Selvester QRS score for electrocardiographic myocardial scar sizing in left bundle branch block. *J Electrocardiol*. 2015.

IV. **Wieslander B***, Loring Z*, Zareba W, McNitt S, Wagner GS, Daubert JP and Strauss DG. Scar burden assessed by Selvester QRS score predicts prognosis, not CRT clinical benefit in preventing heart failure event and death: A MADIT-CRT sub-study. *J Electrocardiol*. 2016;49:603-9.

V. **Wieslander B**, Xia X, Jablonowski R, Axelsson J, Klem I, Nijveldt R, Maynard C, Schelbert EB, Sörensson P, Sigfridsson A, Chaudhry U, Platonov PG, Borgquist R, Engblom H, Couderc JP, Strauss DG, Wagner GS, Atwater BD and Ugander M. The ability of the electrocardiogram in left bundle branch block to detect myocardial scar determined by cardiovascular magnetic resonance. *Manuscript*

(* these authors contributed equally)

CONTENTS

LIST OF ABBREVIATIONS

2009 LBSS	The 2009 Selvester QRS score adapted for left bundle branch block
AHA	American Heart Association
ANOVA	Analysis of variance
AUC	Area under the curve
AV node	Atrio-ventricular node
BNP	Brain natriuretic peptide
BSA	Body surface area
CABG	Coronary artery bypass grafting
CAD	Coronary artery disease
CMR	Cardiovascular magnetic resonance imaging
CRT	Cardiac resynchronization therapy
CRT-D	Cardiac resynchronization therapy and implantable cardioverter defibrillator
CT	Computed tomography
DCM	Dilated cardiomyopathy
DE	Delayed enhancement
DICOM	Digital imaging and communications in medicine
ECG	Electrocardiogram
ED	End diastole
EDV	End diastolic volume
EDVI	End diastolic volume indexed to body surface area
EPV	Events per variable
ES	End systole
FDA	Food and Drug Administration
HF	Heart failure
HR	Hazard ratio
ICC	Intraclass correlation coefficient
ICD	Implantable cardioverter defibrillator
IQR	Interquartile range
IRB	Institutional review board
IVCD	Intraventricular conduction delay
K-S test	Kolmogorov-Smirnov test
LA	Long axis
LAD	Left anterior descending artery
LAFB	Left anterior fascicular block
LBBB	Left bundle branch block
LCX	Left circumflex artery
LGE	Late gadolinium enhancement
LV	Left ventricle
LVEF	Left ventricular ejection fraction
LVH	Left ventricular hypertrophy
LVM	Left ventricular mass
LVMI	Left ventricular mass indexed to body surface area
MADIT-CRT	Multicenter automatic defibrillator implantation trial - Cardiac resynchronization therapy
MAGIR	Magnitude inversion recovery
MI	Myocardial infarction

MRI	Magnetic resonance imaging
NYHA	New York Heart Association
PACS	Picture archiving and communication system
PSIR	Phase sensitive inversion recovery
RBBB	Right bundle branch block
RCA	Right coronary artery
RIS	Radiological information system
ROC	Receiver operating characteristic
RV	Right ventricle
SA node	Sino-atrial node
SD	Standard deviation
SEM	Standard error of the mean
SPECT	Single photon emission computed tomography
TTC	Triphenyl tetrazolium chloride
VCG	Vectorcardiogram

1 INTRODUCTION

The focus of this thesis is the electrocardiographical (ECG) diagnosis of myocardial scar in patients with an abnormally functioning cardiac conduction system. Normally, the innate electrical conduction system within the heart ensures an optimized coordinated contraction of the heart muscle cells, the cardiomyocytes. In particular, a defect in the conduction system known as left bundle branch block (LBBB) can markedly disrupt the heart's ability to pump efficiently. Further, the normal appearance of the ECG is altered extensively when LBBB is present which makes diagnosis of both acute myocardial infarction and chronic myocardial scar challenging. In addition, there is evidence that myocardial scar renders therapies aimed at the remedy of LBBB-induced cardiac dyssynchrony ineffective.
The first chapter of the thesis will discuss the historical development of the ECG until the recent development of a system to derive from it information about scar in patients with LBBB. Further, the genesis and consequences of myocardial scar will be reviewed, as well as current means and importance of diagnosing and characterizing myocardial scar *in vivo*.

1.1 EARLY HISTORY OF ELECTROCARDIOLOGY

The biological role of electricity has been studied during the last centuries in parallel to the long process of discovering electricity itself. Although not the first to discover the generation of electric potentials in the heart, Willem Einthoven was the first to examine the spatial orientation over time of the cardiac electrical potentials to distinguish health from pathology[1]. Using his newly invented sensitive string galvanometer Einthoven measured the voltage differences between different body parts and recorded the results. A publication from 1906[2] contained descriptions of the electrocardiographic (ECG) appearance of several distinct pathologies in a subset of the same ECG leads that are routinely used today.

Figure 1. The normal electrocardiogram

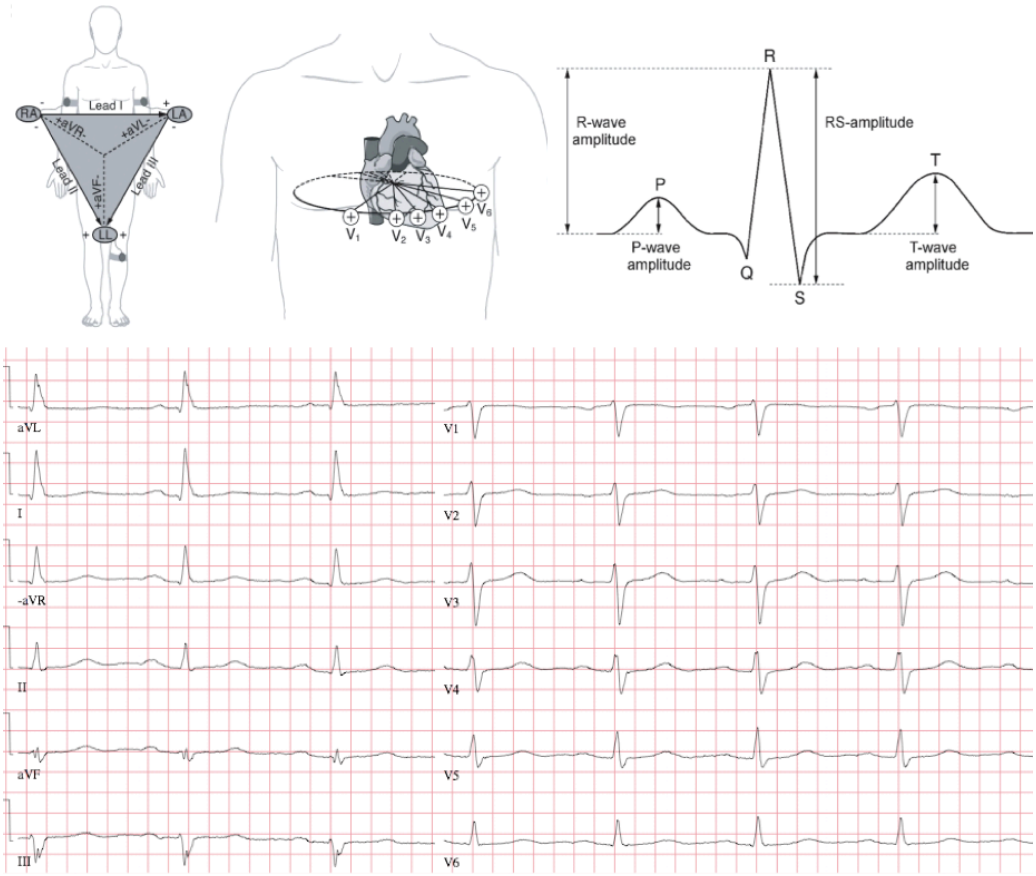

Figure 1: *The spatial directions of the extremity leads I-III and augmented vectors right, left and foot, abbreviated aVR, aVL and aVF, are shown in the upper left panel. The spatial directions of the precordial leads V1-V6 are displayed in the upper middle panel. A schematic representation of the typical electrical signal during one heart cycle is shown in the upper right panel. The P-wave and the QRS complex reflect the depolarization the atria and ventricles, respectively, and the T-wave results from the repolarization of the ventricles. Einthoven changed the waveform denominations from ABCD into letters from the second half to the alphabet, PQRST, to denote that a correction formula had been applied to compensate for the insensitivity of early galvanometers*[3]*. The letters N and O were not used because they had other widely accepted mathematical meanings. The lower panel shows a normal standard 12-lead ECG with limb leads displayed according to the Cabrera sequence*[4] *(aVL, I, -aVR, II, aVF, III), as initially suggested by Fumagalli. The cabrera sequence is routinely used in Sweden among several other European countries. Figure adapted from Koelsch et al*[5] *with permision.*

The construction of a standard ECG was subsequently modified to include nine additional leads through the invention of unipolar precordial leads by Frank Norman Wilson in 1934[6]

and the amplification of these unipolar leads by Emanuel Goldberger in 1942[7]. This expansion resulted in the standard ECG as it is most frequently encountered today (figure 1), which enabled more precise diagnosis of a multitude of cardiac diseases.

In parallel, researchers explored the concept describing the summary of the wavelike spread of electrical activity within the heart as a vector changing over time. Mann became the first to describe the monocardiogram[8], which later came to be known as the vectorcardiogram (VCG). The contribution of the VCG was the more intuitive and direct approach of distinguishing disease from health by the normal or abnormal pattern of the three-dimensional vector loop (figure 2).

Figure 2. Vectorcardiogram

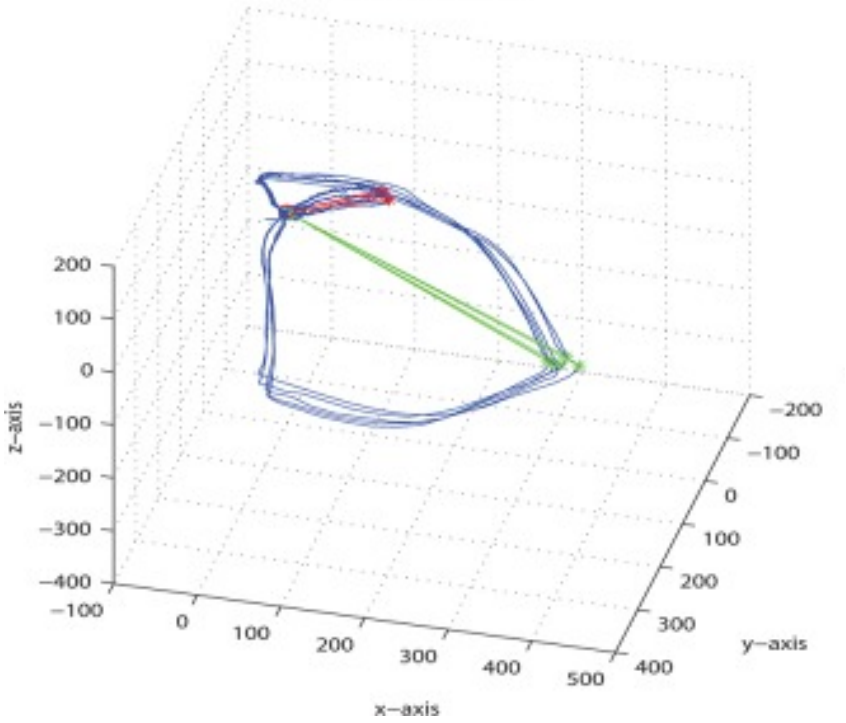

Figure 2. *An example of a vectorcardiogram (VCG). At each measurement of voltage, the potential differences between the leads are used to calculate the magnitude and direction of the net vector of the heart's depolarization in three-dimensional space. As the vector changes over time, its trace forms a "vector loop". In the figure, the blue lines show the vector loops of five ventricle depolarizations. Figure reproduced from Sur et al.[9], with permission.*

This was in contrast to examining waveforms from individual leads which required appreciable spatial imagination on the part of the observer to form a three-dimensional whole picture of the electrical events during the cardiac cycle. Ever since, development and refinement of criteria to discriminate the presence and grade of various disease processes have continued. Both the VCG and the ECG continue to be in use clinically today, although the dominating variation has become the 12-lead ECG shown in figure 1.

1.2 ELECTRICAL CONDUCTION SYSTEM OF THE HEART

In parallel with ECG diagnosis of various diseases being sharpened gradually over the 20th century, the understanding of the cardiac conduction system was being furthered as well. The individual parts of the cardiac conduction system (figure 3) have been characterized both histologically and functionally.

The generation of electrical activity within the heart on a molecular level occurs because cardiac muscle cells, like many other types of cells, have the ability to produce action potentials (figure 4). An action potential is a process during which a cell produces rapid changes of the voltage across the cell membrane. The production of the rapid change of voltage is accomplished by the coordinated opening and closing of ion channels in the cell membrane. This process requires the body to carefully regulate levels of electrolytes such as potassium and sodium in the extra- and intracellular fluid. An action potential can act as a signal to trigger intracellular events, such as muscle fiber contraction, and also to trigger another action potential in an adjacent cell. Cardiac muscle cells, cardiomyocytes, are interconnected electrically through protein complexes termed “gap junctions”[10]. Therefore, an action potential in a single cardiac cell can trigger a wavelike spread of action potentials in

the whole heart by triggering action potentials in its neighbor, which in turn can propagate the action potential to subsequent layers of cells.

Figure 3. Schematic drawing of the electric conduction system of the heart

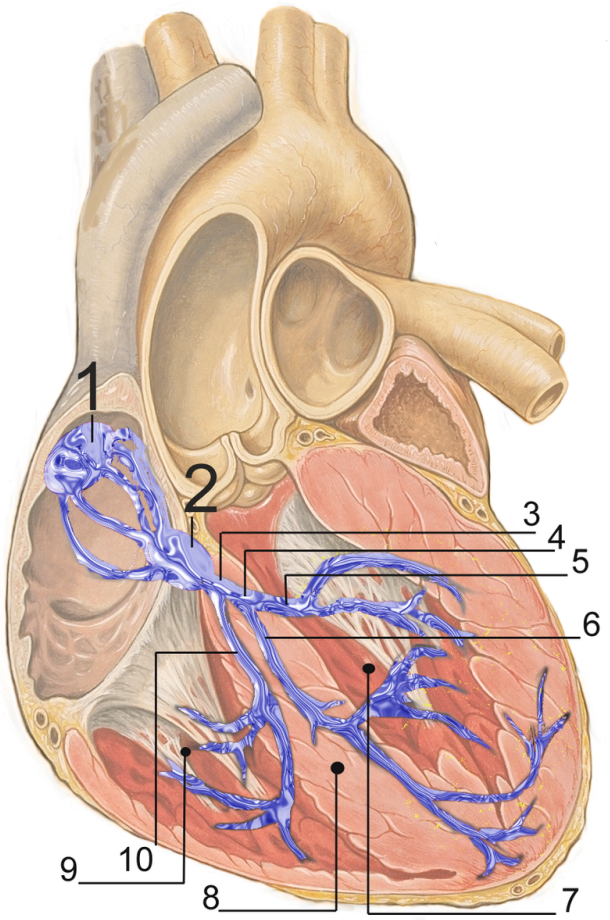

Figure 3. *The principal components of the electrical conduction system of the heart: 1. Sino-atrial (SA) node. 2. Atrioventricular (AV) node. 3. Bundle of His. 4. Left bundle branch. 5. Posterior fascicle of the left bundle branch. 6. Anterior fascicle of the left bundle branch. 7. Left ventricle. 8. Interventricular septum. 9. Right ventricle. 10. Right bundle branch. Figure reproduced under a creative commons license. Original figure by Illustrator Patrick Lynch and cardiologist Carl Jaffe, MD, with subsequent modifications by J. Heuser.*

Specialized cardiac muscle cells that periodically generate action potentials without need for external stimuli were found concentrated primarily in a 10-15 mm by 3 cm area in the upper right atrium close to the coronary sinus (figure 3)[11]. This concentration of cells was termed

the “sino-auricular node” by its discoverers[11]. Today it is more commonly known as the sino-atrial node or SA-node as the word atria has largely replaced the word auricula, which now instead commonly refers to the atria appendages.

Already in 1839 Purkyně described elongated cardiac cells with double nuclei as a distinct feature. These Purkinje fibers were later found through a series of discoveries to have many gap junctions making them suitable for rapid conduction of electric signals more so than contraction. Furthermore, incremental discoveries showed that these Purkinje cells were organized into fibers making up a complex network in the heart, tapering from the bundle branches. Activation spreads throughout the heart in a coordinated fashion through the conduction system thereby yielding an optimized overall contraction to pump out blood to the body efficiently[12]. Key discoveries included the description of the atrio-ventricular bundle named His bundle after its discoverer[13], and the discovery of the atrio-ventricular (AV) node by Tawara in 1907[13].

Figure 4: Myocyte action potential

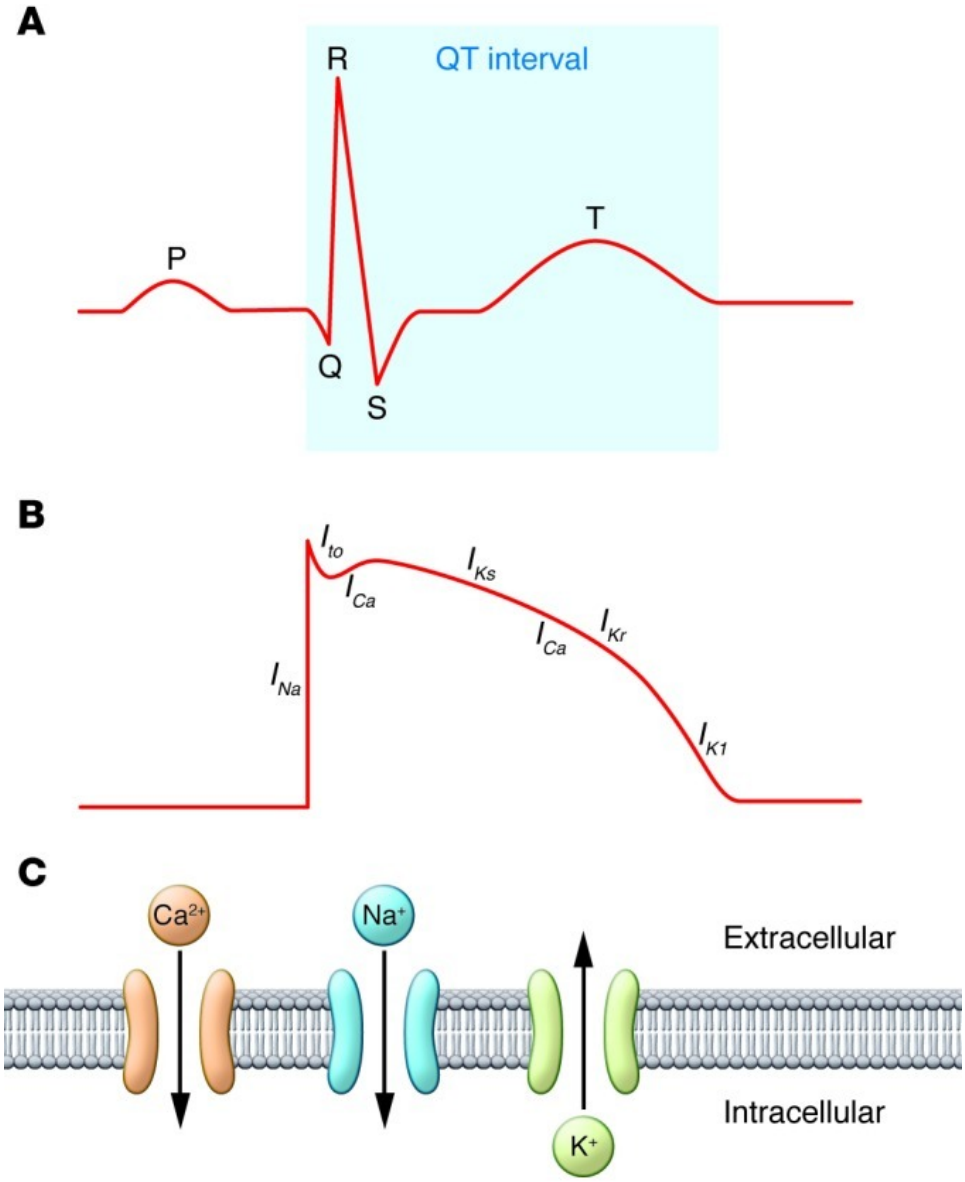

Figure 4. *The temporal relationship between the ECG signal (A), an action potential of a ventricular myocyte (B) and the involved ions flowing across the cell membrane due to the orderly and rapid opening, closure and inactivation of transmembrane ion channels (C). The QRS complex potential differences at the body surface are induced by currents arising from coordinated action potentials in the cardiomyocytes. The letters in panel B reflects the positively charged ions principally involved in different phases of the action potential in a myocyte: the inward sodium (I_{Na}) and calcium (I_{Ca}) currents, and the outward potassium currents (I_{TO}, I_{Ks}, I_{Kr} and I_{K1}). Figure reproduced with from George, et al.,*[14] *with permission conditioned upon provision in this thesis of the publisher's web address:* http://www.tandfonline.com.

More detailed knowledge of the conduction in the human heart emerged from remarkable experiments conducted by Durrer et al[15], where healthy human hearts were collected from

accident victims and suspended outside the body. Durrer implanted needles into each collected and suspended heart according to a coordinate system in order to map out the exact sequence of activation of the heart muscle. The results were highly detailed maps of the activation sequence of the collected hearts (figure 5), which later served as basis for the development of the Selvester QRS score described in a later section of this thesis.

Figure 5. Durrer's myocardial activation maps

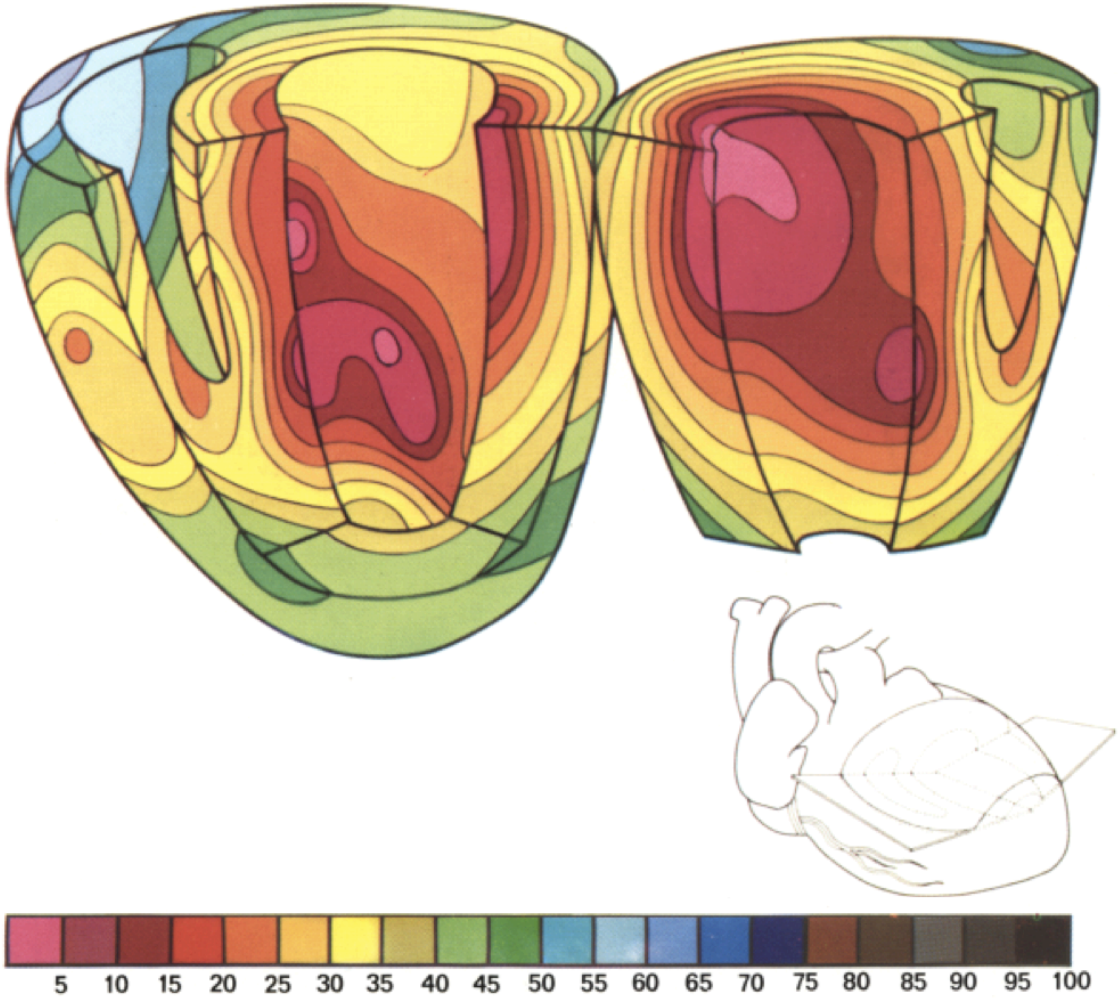

Figure 5. *Transmural myocardial activation maps showing which myocardial areas activate simultaneously (isochrones). Timing of activation is color coded, with the colors corresponding to milliseconds from start of activation according to the scale at the bottom. Notably, the activation starts in the endocardium of three sites in the left ventricle, one anterior, one posterior and one septal, corresponding to the most common anatomical configuration of three branches of the left bundle branch. Reproduced from Durrer, et al.,*[15] *with permission.*

1.2.1 Conduction abnormalities

Einthoven[16] described in his 1925 Nobel lectures a patient with an unusually broad QRS complex thought to represent a blockage of the left bundle branch. Since then, ECG criteria have evolved[17] for blockages at various sites in several combinations and the most commonly used are described in recent guidelines of the American Heart Association (AHA)[18]. However, the criteria for several different conduction abnormalities still continue to evolve. Recently, new stricter criteria for left bundle branch block (LBBB) have been published by Strauss, et al,[19] based on invasive electrophysiological measurements by Auricchio and colleagues[20]. Importantly, there is a sizeable inter-individual anatomical variation in the conduction system downstream from the bundle of His[21], as shown in figure 6. These variations likely impact the effects of blocks at various levels of conduction system upon the ventricular depolarization reflected in the QRS complex of the ECG. Despite this heterogeneity, several distinct categories of conduction abnormalities have been characterized according to ECG appearance, as described below.

Figure 6. Anatomical variations of the left bundle branch

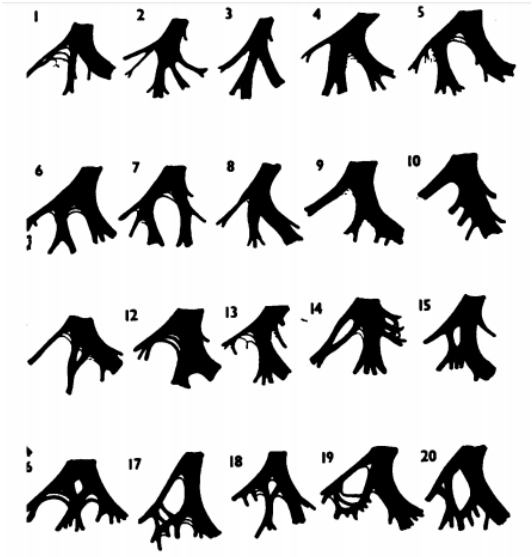

Figure 6. *The sketches show reconstructions of the left bundle branch anatomy from twenty human hearts, illustrating the anatomical heterogeneity of the conduction system. Reproduced from Demoulin, et al.,[22], with permission.*

1.2.1.1 Left bundle branch block

As the name suggests, LBBB denotes a condition in which conduction in the left bundle branch is absent. This markedly alters the LV activation pattern. Instead of near simultaneous multisite activation as shown in Durrer's maps in figure 5, the LV is activated from the right side of the septum to the lateral wall in a sequential manner as shown in figure 7, panels A and B. This tends to result in a significant delay in the activation of the lateral wall that can be visualized in by functional CMR imaging as shown in figure 7, panel C.

As shown in figure 7, panel A, the ECG typically reflects this altered activation pattern by a deep broad terminal negative deflection in leads V1 and V2. There has been some evidence that other cardiac causes may mimic this ECG appearance as demonstrated by Strauss[19], who suggested the following alternate criteria: terminal negative deflection in lead V1, QRS duration of ≥130 ms for women and ≥140 ms for men and presence of mid QRS notching or slurring. The notching or slurring in the mid-period of the QRS complex is thought to result from a change of wavefront direction occuring when the right-to-left activation of the septum reaches the LV endocardium. Invasive catheter measurements[23] have shown that patients meeting traditional LBBB criteria as described by the AHA[18] are readily divided into two distinct cohorts that have an LV endocardial activation time of longer than or clearly shorter than 40 ms[23].

In principle, any myocardial disease process affecting the left bundle may cause LBBB. Cardiac disease and age[24] have been found to be the greatest risk factors for developing it. Known causes, other than cardiomyopathies in general, include selective calcification of the conduction system[25] and surgical repair of the aortic valve[26]. It has been shown that patients with cardiomyopathy and LBBB are less likely to have had a large anteroseptal infarction than patients with RBBB[27], suggesting that the left bundle is less vulnerable to occlusion of the left anterior descending (LAD) artery. Prognostically, LBBB has shown to be an adverse sign[28, 29].

Figure 7. Electrical and mechanical delay of the left ventricular lateral wall in LBBB

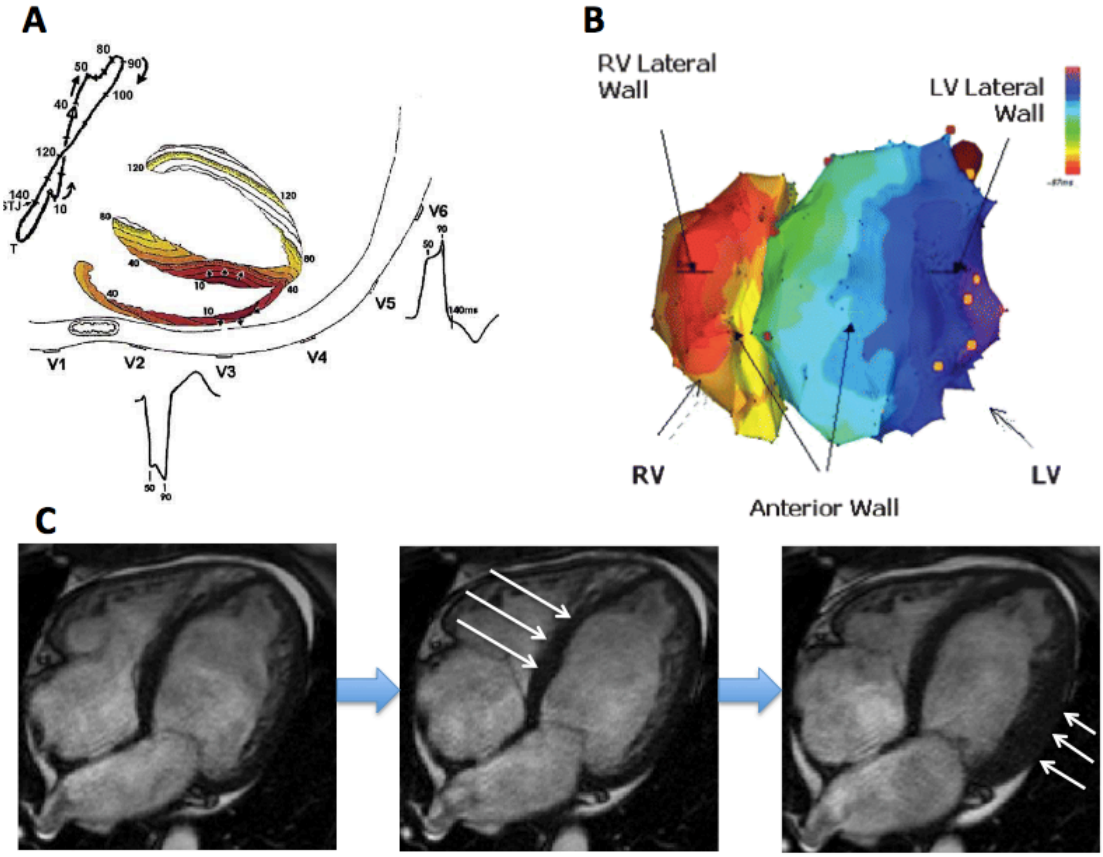

Figure 7. *Panel A: A schematic model of the activation pattern of the heart in presence of left bundle branch block (LBBB), with areas of the same color being activated within the same 10 ms (isochrones). The resulting vector loop (upper right) and QRS complex appearance in the precordial leads is shown. Noticeably, sequential activation of the left ventricle (LV) from the right side of the septum gives rise to a leftward and posteriorly directed activation wavefront causing the characteristic negative deflection in the septal leads V1 and V2 and positive deflections in the lateral leads V5 and V6. The mid-QRS notch required by the Strauss criteria for LBBB[19] is thought to reflect the change of wavefront direction resulting from septal breakthrough of activation to the septal LV endocardium. Panel B: An endocardial map obtained through catheterization, with color-coded isochrones showing the delayed electrical activation of the blue colored lateral LV wall. Panel C shows functional cine CMR images from an LBBB patient in study V in four-chamber view. The three timeframes shown highlight the initial activation of the septal wall in the middle image followed by contraction of the lateral wall in the far right image. Panels A and B are adapted from Strauss, et al.[30] and Fantoni, et al.[23], respectively, with permission. Abbreviations: LV = left ventricle. RV = right ventricle.*

1.2.1.2 Other conduction abnormalities

Beyond LBBB, there are multiple other specific conduction abnormalities with individual pathophysiologies, prognostic significance and ECG criteria. These include right bundle branch block (RBBB), left anterior and posterior fascicular blocks (LAFB and LPFB, respectively), non-specific intraventricular conduction delay (IVCD), several types of atrio-ventricular (AV) block as well as combinations of the above. The AV-block types disrupt the connection between the atria and the ventricles to a varying degree, and their pathophysiology and effects fall outside the scope of this thesis. The other conduction abnormalities largely share causes with LBBB. It has been found that RBBB is associated with the presence of large anteroseptal infarction[27] in patients with cardiomyopathy to a higher degree than LBBB. This suggests that the right bundle is more vulnerable to ischemic injury due to anatomical reasons. Although patients with HF and other conduction abnormalities than LBBB do not seem to respond well to CRT[31], both RBBB and LAFB have been shown to carry prognostic significance with regards to mortality and morbidity[32-34].

1.3 HEART FAILURE

The normal function of the heart is to pump sufficient blood to meet the metabolic demands of the body. Heart failure (HF) is said to occur when the heart can no longer perform this function. The prevalence of HF is high world wide, particularly in the developed world with an estimated lifetime risk of 20% for Americans under 40 years of age[35]. Furthermore, prognosis for those affected is comparable to many malignant diseases with approximately 50% mortality within 5 years of diagnosis[35].

Although inability to meet the body's perfusion demand is a seemingly simple definition, it is not always easy to objectively determine whether HF is present in practice. The AHA state in their 2013 HF management guidelines that: *"There is no single diagnostic test for HF*

because it is largely a clinical diagnosis based on a careful history and physical examination"[35]. Yet, there are clinical signs, laboratory tests and imaging methods that can help the clinician to elucidate whether the hallmark symptoms of HF such as shortness of breath and fluid retention are due to malfunction of the heart or something different. Clinical signs include the aforementioned hallmark symptoms, swelling of the legs, abdomen and/or neck veins and crackles upon lung auscultation. The most utilized laboratory test in diagnosing and grading HF is blood level of brain natriuretic peptide (BNP), a compound released by cardiomyocytes when cardiac muscle tissue is stretched, e.g. because of volume overload[36]. Imaging and other investigative modalities used clinically in determining presence of HF or its many causes include ECG, echocardiography, cardiac magnetic resonance imaging (CMR) and myocardial scintigraphy, with or without exercise/pharmacological stress, as well as invasive heart catheterization.

Heart failure has many causes, all of which impair the heart's ability to pump blood. A detailed review of these causes, their pathophysiologies and appropriate treatments falls outside the scope of this thesis, but an overview of cardiomyopathies that can cause HF is displayed in figure 8. Causes that more often result in myocardial scarring are described in more detail below.

A widely used scale to grade the severity of HF is the New York Heart Association (NYHA) functional classification (table 1)[37].

Table 1. New York Heart Association functional classification

Class	Patient Symptoms
I	No limitation of physical activity.
II	Slight limitation of physical activity. Comfortable at rest.
III	Marked limitation of physical activity. Comfortable at rest.
IV	Unable to carry on any physical activity without discomfort. Symptoms of heart failure at rest.

Figure 8. Overview of cardiomyopathies and treatment of heart failure

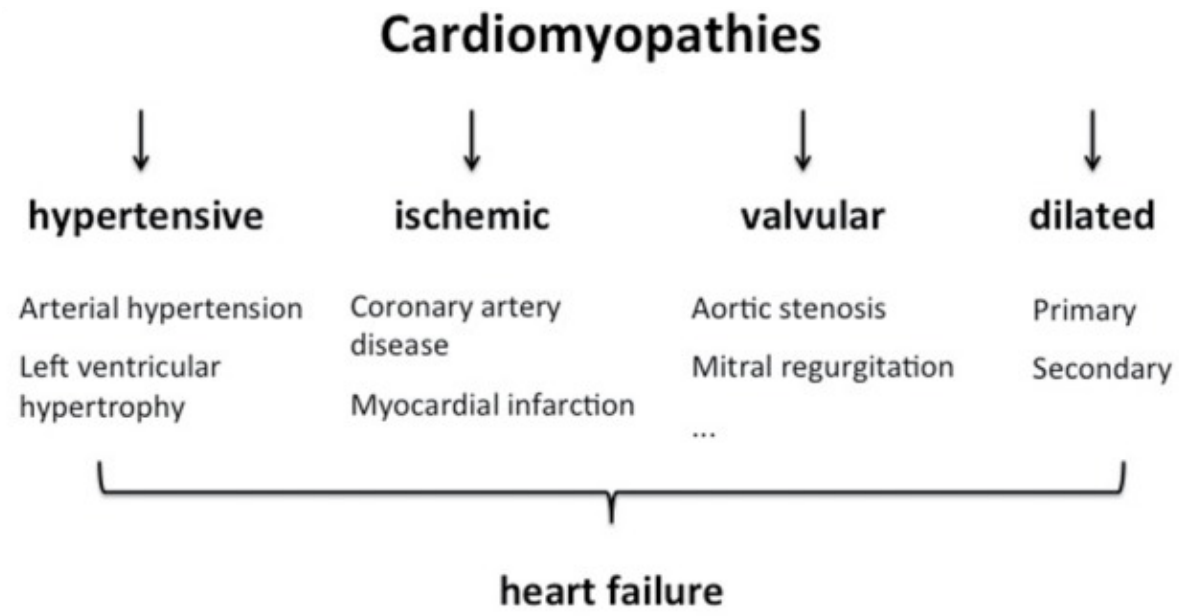

Figure 8. *Summary of broad categories of cardiomyopathies causing HF. Reproduced from Drazner, et al.,[38] with permission.*

1.4 MYOCARDIAL SCAR

When human myocardium is damaged, it is typically replaced by fibrous tissue, comprised mainly of collagenous extracellular matrix and fibroblasts. When the fibrotic process is focal, the resulting area of fibrous tissue is commonly referred to as myocardial scar. Myocardial scar cannot contract and thus cannot contribute to myocardial function.

1.4.1 Causes

There are several mechanisms through which healthy myocardium may be damaged and subsequently replaced by myocardial scar. These mechanisms are frequently divided into ischemic (infarction) and non-ischemic causes, and the latter category includes myocarditis, hypertrophic cardiomyopathy and dilated cardiomyopathy, among many others[39].

1.4.1.1 Ischemic etiology of myocardial scar

Cardiac ischemia occurs when the heart itself is deprived of the blood flow it needs in order to function normally. When ischemia is severe and lasts for hours or more, cardiomyocytes undergo necrosis from the endocardium and outward, and acute myocardial infarction is manifest. The typically decades long pathophysiologic process of coronary atherosclerosis preceding myocardial infarction creates conditions conducive to complete coronary occlusion, often caused by plaque rupture and clot formation. Myocardial infarction can also occur when coronary blood flow is restricted by protracted coronary spams or if the capability of the blood stream to deliver oxygen is impaired for other reasons such as severe hemorrhage or anemia.

1.4.1.2 Non-ischemic etiologies of myocardial scar

As HF progresses, the end stage is typically a state of dilated cardiomyopathy (DCM) in which the heart's walls are thinned out and the heart chambers are enlarged. At this stage, the normal orderly arrangement of cardiomyocytes can get disrupted on a histological level[40] and patches of myocardial scar can appear throughout the cardiac muscle tissue. In particular, this type of scarring tends to occur at sites exposed to mechanical stress such as the insertion points of the right ventricular (RV) walls (figure 9). Beyond these patchy areas of scar that tend to appear as dilation of the heart progresses in HF, there are other non-ischemic processes that can give rise to myocardial scar in other ways, summarized in figure 9. These include but are not limited to inflammatory and infectious cardiomyopathies such as sarcoidosis, viral myocarditis and Chaga's disease. Furthermore, characteristic patterns of scarring can be seen in left ventricular hypertrophy (LVH) preceded by longer periods of increased load, such as in the presence of hypertension or valvular disease.

Figure 9. CMR-LGE: characteristic patterns of hyperenhancement of various cardiomyopathies

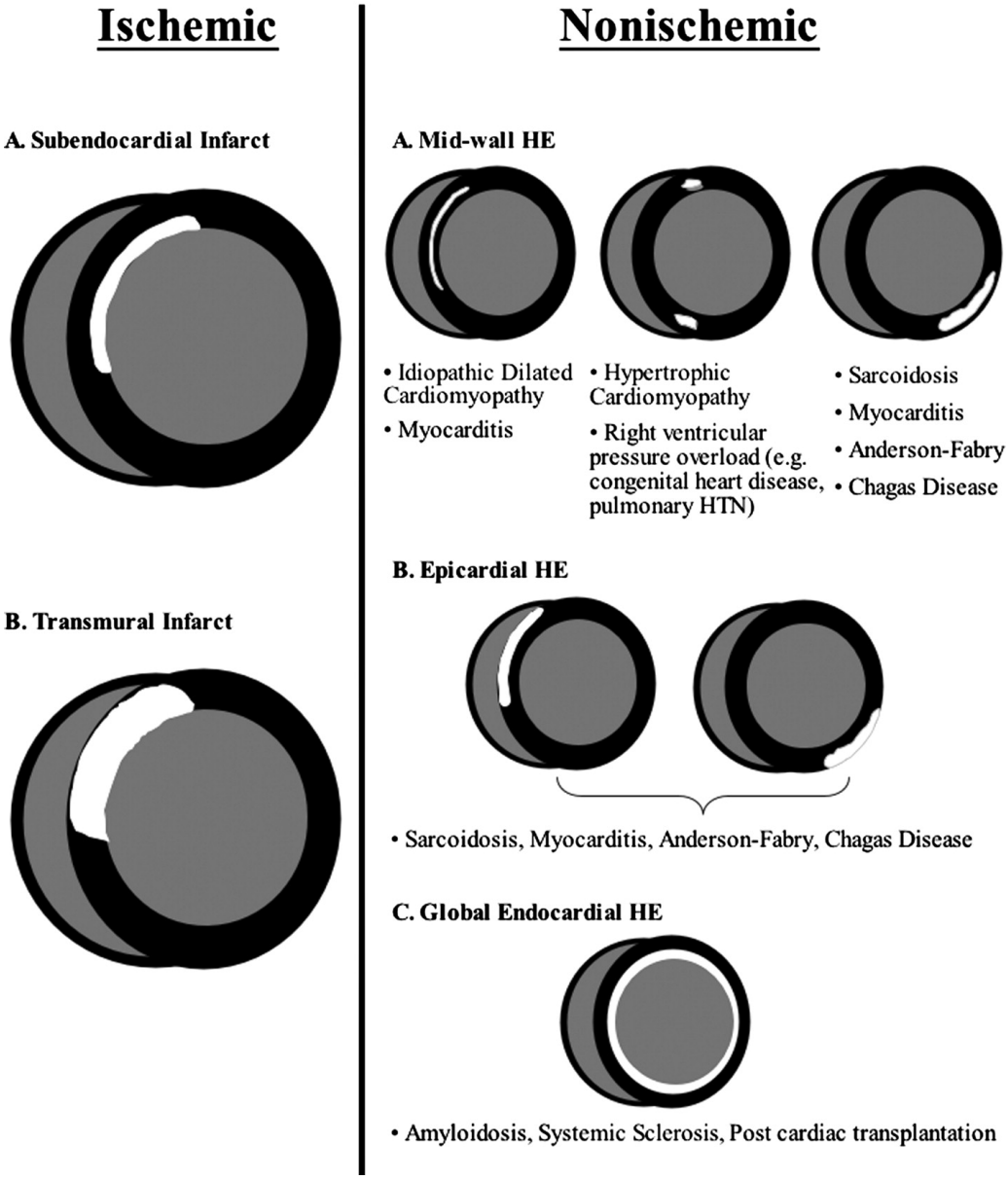

Figure 9. *Schematic overview of patterns of hyperenhancement on CMR images with late gadolinium enhancement (LGE) typically associated with various cardiomyopathies known to cause myocardial scar. Reproduced from Mahrholdt, et al.[39], with permission. Abbreviations: HE – Hyperenhancement.*

1.4.2 Consequences

Patients with myocardial scar as determined by CMR with late gadolinium enhancement (LGE) have poorer prognosis than those without, especially if the etiology of the scar is

ischemic[41-45]. There are several reasons for this, including but not limited to the mechanisms described below.

1.4.2.1 Loss of cardiac function

After cardiomyocytes undergo necrosis they are typically replaced by inelastic fibrous tissue, referred to as scar, consisting of fibroblasts and extracellular matrix comprised mostly of collagen[39]. Scar has different properties than normal myocardium in that scar tissue cannot conduct electrical signals well and cannot contribute to myocardial function, thereby leading to loss of contractile ability.

1.4.2.2 Disruption of normal activation

Beyond the loss of contractile ability due to loss of functioning cardiomyocytes, areas of myocardial scar may also disrupt normal electrical and mechanical activation patterns of the heart. This can lead to a suboptimal activation of the remaining viable myocytes in terms of the ability to optimally generate systolic function. Furthermore, inferior infarcts in particular may interfere with ability of the SA node to generate a regular rhythm and may also affect conduction over the AV node[46].

1.4.2.3 Arrhythmic substrate

Electrophysiological studies have found that potentially deadly ventricular arrhythmias often originate from areas of myocardial scarring and can often be successfully prevented by ablation of remaining interspersed healthy cardiomyocytes in and around the scar tissue. These surviving cardiomyocytes can constitute a threat because they may get triggered into depolarizing at irregular intervals and by providing slow conducting pathways for re-entry phenomena to occur[47]. Moreover, a major cause of death early after a myocardial infarction is ventricular arrhythmias, with the highest risk occuring during the first few days after infarction[46].

1.4.2.4 Decreased response to device therapy

Cardiac resynchronization therapy (CRT) is a device therapy aimed at partially restoring a normal electrical activation pattern in patients with a dyssynchronous cardiac contraction[48]. Myocardial scar at the site of implantation of the LV lead tip has been shown to dramatically decrease the effectiveness of CRT[48].

1.4.3 Importance of diagnosis

Presence and extent of myocardial scar may affect choice of treatment, particularly in patients with heart failure[41, 45, 49]. Increased scar extent heralds poor prognosis[41, 44, 45], poor left ventricular ejection fraction (LVEF)[50], increased risk of ventricular arrythmias[47, 51] and poor response to CRT[52-54]. In addition, localization of myocardial scar affects prognosis in patients who receive CRT[48, 52, 54]. The clinical finding of myocardial scar may also warrant different secondary preventive treatment strategies depending on its cause. Different treatment strategies are prudent for a patient with a previous infarction versus a patient with myocardial scar due to myocarditis.

1.4.3.1 Unrecognized myocardial scar is prevalent and dangerous

Unrecognized myocardial infarction (MI) is common. One study found that among 599 randomly selected Icelandic elderly participants (67-93 years of age) without diabetes, there were 54 (9%) who had a clinically recognized MI and another 85 (14%) who had previously unrecognized MI[55]. Corresponding numbers in 337 patients with diabetes were 37 (11%) with recognized MI and another 72 (21%) with unrecognized MI[55]. In addition, the patients with unrecognized MI were found to have less cardiac medication than patients with known MI, and a higher risk of death per unit of time with a hazard ratio (HR) of 1.45 versus patients with no infarction, independently of age, gender and diabetes[55]. These numbers included only MI and did not take into account myocardial scar patterns consistent with non-ischemic etiology, which have been shown in other studies to be associated with

poor prognosis in patients with HF of non-ischemic etiology[41, 45]. In different study, n=1840 somewhat younger US participants without a known history of coronary artery disease (CAD) underwent CMR at ten years after baseline (mean age 69 at CMR)[56]. The study found that non-ischemic scar was as prevalent as ischemic scar (4.1% and 3.8% prevalence, respectively).

1.4.3.2 Impact of scar on response to device therapies

Several studies have found that scar burden estimated either by CMR LGE[49], SPECT-estimated perfusion defect[57] or ECG[58-60] is associated with poor response to CRT. The aim of CRT is to resynchronize the heart's walls when a conduction abnormality causes mechanical dyssynchrony. Already in 1968, adverse effects of abnormal activation induced by RV apical pacing were found by Kowolsky et al[12]. The activation sequence of the LV during RV pacing share similarities the pattern in LBBB[61]. The results is a delayed activation of the lateral wall of the LV, which causes dyssynchrony visible in functional cardiac imaging, e.g. by CMR as shown in figure 7, panel C. This dyssynchrony is partially corrected in CRT by insertion of two ventricular pacing electrodes, one in the traditional RV apical position and another in the LV lateral wall[62], resulting in a more synchronous LV activation as shown in figure 10. Therefore, when there is scar in the LV lateral wall at the site where the LV pacing electrode lead tip is implanted, the scar may act as an insulator and prevent myocardial depolarization from following a pacing impulse[54]. Therefore, both scar burden and localization may impact CRT response.

Recently, the alternative option of His bundle pacing has been gaining ground as a means to utilize the existing Purkinje fiber network to restore the natural multisite activation sequence. This technique is currently being explored and the procedural details are being refined. His bundle pacing often reverses the distinct ECG appearance of LBBB completely, indicating that the block can often be overcome to employ the existing Purkinje network to a great extent[63]. In addition, a recent study has shown that patients with LBBB and mild HF

symptoms have a higher risk of heart disease[28], suggesting the importance of avoiding extended time periods of stress on the heart induced by a suboptimal activation sequence. This notion is also supported by the finding of adverse effect on myocardial function after long durations of RV pacing[64]. One study has shown that the combination of His bundle pacing and traditional CRT has favorable hemodynamic properties over CRT alone, demonstrating that it is beneficial to even partly recruit the native Purkinje network[65].

Finally, presence and extent of myocardial scar has been shown to predict who benefits from treatment with implantable cardioverter defibrillator (ICD)[51, 66]. This finding is in line with the concept of myocardial scar as an arrhythmogenic substrate described above.

Figure 10. Endocardial mapping of activation sequence during LBBB with and without biventricular pacing.

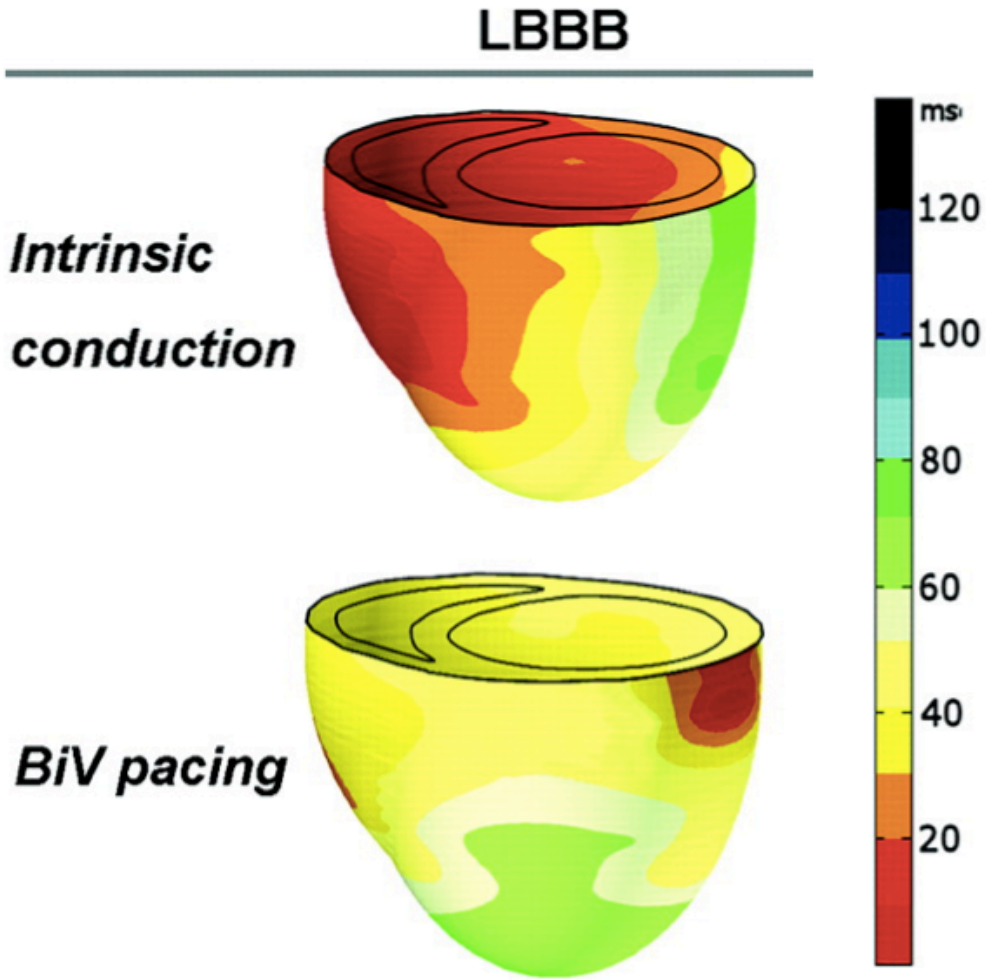

Figure 10. *The decreased delay in activation of the lateral wall during biventricular pacing is visualized by endocardial mapping, showing activation sequence in representative canine hearts with LBBB. Areas of same color are activated near simultaneously (isochrones), at the time from start of activation indicated by the color-scale to the right. Abbreviations: LBBB – Left bundle branch block. BiV pacing – biventricular pacing. ms – milliseconds. Reproduced and adapted from Rademakers, et al.*[67]*, with permission.*

1.5 DETECTION OF MYOCARDIAL SCAR

There are multiple methods aimed at detecting the presence, causes and consequences of myocardial scar. All of these methods have particular roles to play in clinical routine care. The most commonly used methods are summarized in this section, apart from the ECG which is described in greater detail later in this thesis.

1.5.1 Cardiovascular magnetic resonance imaging with late gadolinium enhancement

Magnetic resonance imaging (MRI) utilizes the effect of strong and rapidly changing magnetic fields upon the spinning of hydrogen nuclei in the body, and is generally an excellent method to image soft tissues. The main advantage of the method is highly accurate imaging without need for ionizing radiation. However, MRI is relatively costly and requires specially trained operators to ensure high image quality and patient safety. The MRI scanner can acquire images with many different properties using various pulse sequences. These are preprogrammed descriptions detailing timing, magnitude and spatial direction of changes in magnetic fields and radio frequency pulses, as well as timing of data acquisition. The preferred category of pulse sequences to image myocardial scar are referred to as LGE or delayed enhancement (DE) sequences, during which data is acquired 10-15 minutes after administration of a gadolinium-based contrast agent[68, 69]. The rationale for this is that intravenously administered gadolinium-based contrast agents distribute into the body's extracellular space but do not enter living cells. Because areas of myocardial scar consist of large amounts of collagen interspersed with small and elongated fibroblasts, myocardial scar has a much higher proportion of extracellular volume fraction[68, 70]. As a consequence, contrast is found in higher concentration in areas with myocardial scar compared to healthy myocardium. Gadolinium heavily influences the magnetic property T1 of a given tissue, which is the rate at which a proton returns to its their original spinning direction in the

magnetic field of the scanner after having been temporarily influenced by a radio frequency pulse. Therefore, images where signal intensity is primarily influenced by T1 can be used to differentiate areas with high and low extracellular volume fractions such as scar and myocardium. An example of an LGE image is shown in figure 11.

Figure 11. CMR-LGE images from a patient in study V with a transmural inferior infarction.

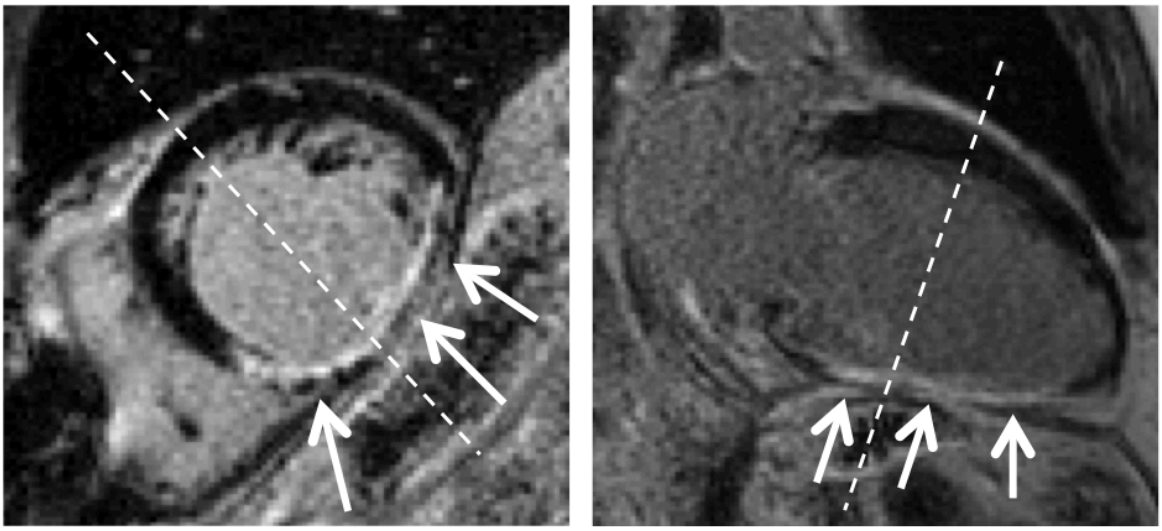

Figure 11. *The left panel is short axis CMR-LGE image from a patient in study V with evidence of transmural infarction in the inferior wall (white arrows), clearly distinguishable from the dark healthy myocardium. The right panel is a long axis 2-chamber view in which the presence of white hyperenhancement can be confirmed in the inferior wall (white arrows). The dashed lines show where the respective image planes of the left and right panels intersect.*

1.5.2 Echocardiography

Echocardiography cannot be used to directly differentiate between myocardial scar and healthy myocardium but can still detect typical functional and morphologic changes associated particularly with ischemic scar. Myocardial infarctions typically result in marked wall thinning (as is visible in figure 11). Furthermore, Tissue Doppler based echocardiograpic parameters can be used as a quantitative way of differentiating between non-contractile

myocardial scar and healthy myocardium by assessing wall motion[71]. Echocardiography requires less expensive equipment than CMR, is less cumbersome and similarly to CMR does not entail exposure to ionizing radiation. However, echocardiography does not allow tissue characterization with the same accuracy as CMR and is more dependent on a skilled observer to reproducibly interpret images[71].

1.5.3 Myocardial scintigraphy

Single photon emission computed tomography (SPECT), also known as myocardial scintigraphy, involves injecting a radioactive tracer into the bloodstream. The tracer is taken up by tissue in proportion to both mitochondrial content and perfusion, and the radiation from the tracer is subsequently detected to produce tomographic images. The advantage of the method is the ability to map out the relative perfusion within the heart during rest, exercise or pharmacological stress. Consequently, myocardial scintigraphy is unable to identify areas with non-ischemic scar as well as areas of scar with restored perfusion. However, the technique is highly useful in determining whether coronary artery stenosis is present without need for invasive catheterization. Still, some studies use resting SPECT as a reference standard identifying myocardial scar[57].

1.5.4 Coronary angiography

Coronary angiography involves inserting intraarterial catheters and manipulating them to reach the coronary arteries. The procedure is not without risk, but has great diagnostic and therapeutic utility in detecting and opening up stenoses in coronary arteries. In order to visualize the blood vessels during the procedure, a contrast agent is injected as moving x-ray images are obtained (fluoroscopy).

1.5.5 Computed tomography

Cardiac computed tomography (CT) can be performed using late enhancement imaging with iodinated contrast agents. The same basic technique of performing imaging between 5-15 minutes after administration of contrast is employed for both CT and CMR. Myocardial scar identified by cardiac CT correlates well with both CMR-LGE and pathology[72-75]. However, the contrast to noise ratio for myocardial scar by late enhancement CT is far lower than for CMR, thus rendering late enhancement CT less useful in clinical routine.

1.5.6 Post mortem examination

Histologic and/or macroscopic examination of hearts from deceased patients can reveal areas of myocardial scar by applying tetraphenyl tetrazolium chloride (TTC) dye[76]. Application of TTC results in macroscopically clearly visible myocardial scar which allows for rigorous validation of novel techniques to image myocardial scar. It has been demonstrated the CMR-LGE images correlate well with infarcted areas by post mortem examination with TTC[68].

1.6 ELECTROCARDIOGRAPHIC DIAGNOSIS OF CHRONIC MYOCARDIAL SCAR

The 12-lead ECG is a highly useful method to detect acute ischemia by assessment of repolarization disturbances visualized in the ST segment (as shown in figure 12). The ECG can also in many cases detect past myocardial infarction and other types of myocardial scar, which is the focus of this thesis. Using the standard 12-lead ECG, localized loss of electrical forces due to infarction can be visualized. In the absence of conduction abnormalities, this loss of activation typically manifests as pathological Q-waves as shown in figure 13 and loss of R-wave amplitude in certain leads depending on the localization of the diseased myocardium. These observations have been made in many different studies, which has resulted in a wide array of ECG criteria for myocardial scar. One attempt at

consolidating ECG criteria for a wide range of diseases is the Minnesota code[77]. Another is a series of attempts at standardizing ECG interpretation through a series of publications by the AHA[18, 78-82]. Perhaps because the ECG has been around for so long as a common diagnostic method, there are many misconceptions around the connections between certain ECG patterns and the properties and presence of myocardial scar among doctors and health professionals world wide. One such misconception is that the ECG can reliably discriminate between transmural and subendocardial infarctions by the presence or absence of Q-waves (figure 13). A recent study comparing ECG and CMR found that pathological Q-waves appear in 8% of patients without MI, in 50% of patients with subendocardial infarction and 72% with transmural infarction[83]. A different ECG analysis method that focuses solely on detection of chronic myocardial scar is the Selvester QRS score described below.

Figure 12. ECG with ST-elevation induced by acute myocardial ischemia

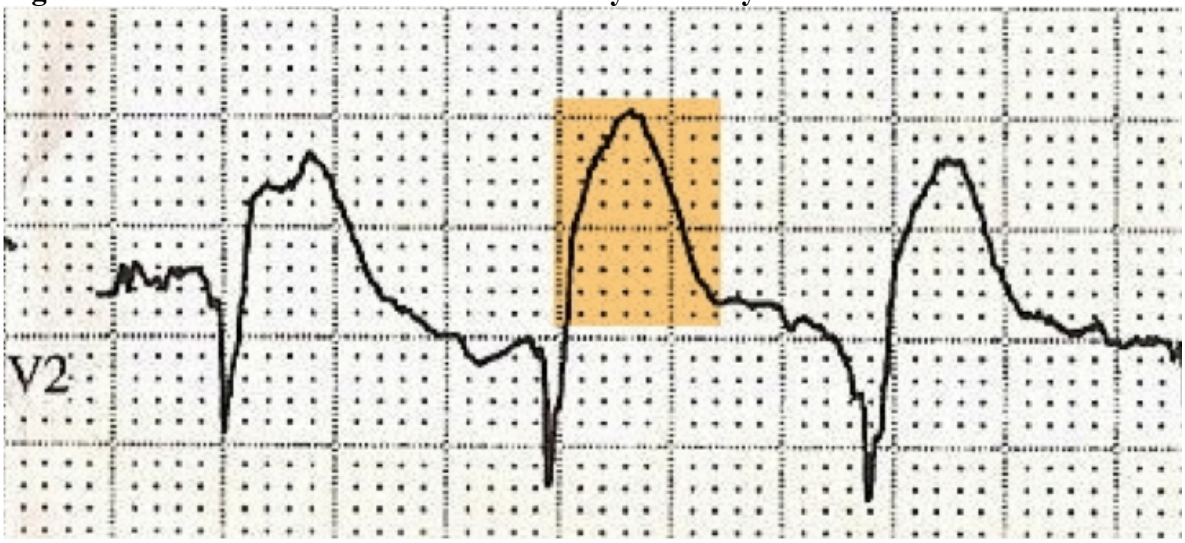

Figure 12. *The figure shows the typical ECG sign of acute myocardial ischemia threatening imminent myocardial infarction. The T-wave (yellow square) starts immediately after the QRS-complex high above the baseline, making the QRS-complex and T-wave hard to separate. In a healthy patient, the ST-segment between the QRS-complex and the T-wave is normally flat and in level with the baseline as shown in figure 1. Furthermore, the absence of the normally present R-wave in lead V2 indicates a loss of depolarizing myocardium in the anteroseptal wall. Figure is public domain and can be reproduced for any purpose without permission.*

In addition, pathological processes that lead to myocardial scarring may affect the conduction system and the pacemaker function of the heart. These effects include RBBB caused by septal infarction[27] and impairment of AV- or SA-node function typically caused by right coronary artery occlusion[46].

Figure 13. Schematic illustration of Q-waves

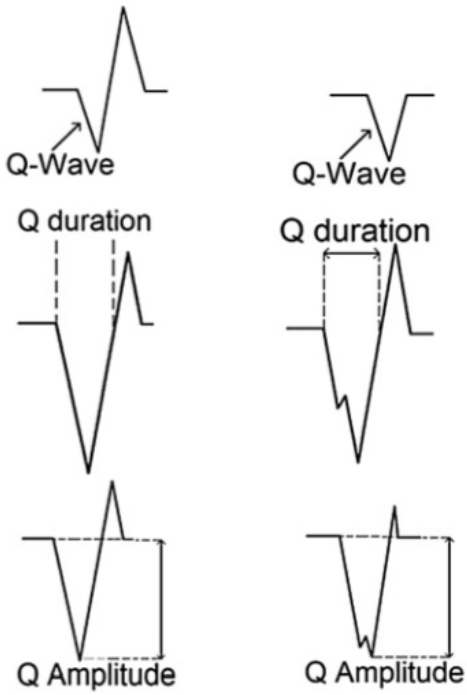

Figure 13. *A Q-wave is a negative deflection at the start of the QRS-complex. In most leads, the QRS-complex normally starts with a positive deflection as in the normal ECG shown in figure 1. Myocardial infarction and other pathological processes can lead to localized loss of healthy myocardium, which in turn decreases spread of depolarization in certain directions. This may in turn cause decreased R-wave amplitude or even appearance of abnormal Q-waves in certain leads relative to localization of the lost myocardium. In general, deeper and wider Q-waves are thought to indicate greater loss of healthy myocardium. Figure reproduced from Loring, et al.,[84] with permission.*

1.7 SELVESTER QRS SCORE

1.7.1 Original Development

The Selvester QRS score is an ECG scoring method that aims to detect, quantify and localize myocardial scar through analysis of QRS complex morphology[30]. The original version of it was developed in the 1970's based on computer simulations that were in turn based on the pioneering experiments by Durrer et al described above[15, 85-92]. The Selvester QRS score was designed to only be used in the absence of conduction abnormalities that change the appearance of the ECG such as LBBB, right bundle branch block (RBBB), left anterior fascicular block (LAFB) and electrocardiographic LVH[30]. The basic method of developing the Selvester QRS score was careful study of the impact on myocardial scar in different regions of the heart upon the ECG appearance in computer simulations, which Selvester then used to construct ECG criteria for presence of myocardial scar[30]. Next, these ECG criteria were consolidated into a unified scoring system. The more criteria a patient met, the larger the myocardial scar was hypothesized to be. Selvester also sought to make predictions about scar location and size by translating the specific criteria into points. These points were in turn translated into certain quantities of scar distributed into twelve myocardial regions, as shown in figure 14. Over the next decades, the criteria comprising the Selvester QRS score were evaluated against myocardial scar found and quantified during post mortem pathologic examinations. During this process, the criteria were incrementally refined to improve diagnostic performance. A limitation with this method was the amount of work involved in each post-mortem examination, which limited the size of datasets in which the Selvester QRS score could be refined and validated. Another limitation was that additional infarction could theoretically have developed in some patients in between the last available 12-lead ECG and the time of death. Later comparison during the 2000's between anterior infarct size by Selvester QRS scoring and by CMR-LGE[93] showed a modest correlation between the two methods (r=0.40). Although it was for a time

one of the easiest, most accessible and accurate ways to non-invasively image myocardial scar, the Selvester QRS score never achieved widespread clinical use. One reason for this may be the relatively cumbersome application, with need for careful measurements of a multitude of ECG waveforms, followed by calculation of the overall score. Efforts to automate the score have been made[94] but have not been widely implemented. Another reason why the Selvester QRS score never became widely used may be because perceived lack of incremental clinical utility beyond the classical signs of chronic MI in the Minnesota code, such as pathological Q-waves.

1.7.2 Adaptation for conduction abnormality

Despite the limitations described above, the prospect of identifying, quantifying and localizing myocardial scar using the ECG saw new interest late in the first decade of the 2000's as it became apparent that scar had a role in the 30% non-response rate to CRT[31, 62, 95-97]. The ECG was found to be a key predictive method and it soon became clear that patients with LBBB were the group with highest response rate[96, 98]. Thus, Selvester and Strauss adapted the Selvester QRS score for use in the presence of various conduction abnormalities. The new adapted versions of the Selvester QRS score were published in 2009[30] and were designed to take into account the altered myocardial activation pattern in the presence of the following conduction abnormalities: LBBB, RBBB, LAFB, LVH and the combination of RBBB+LAFB. The LBBB version is shown in figure 15 and the other conduction types are shown in figure 14. Prior to the work described in this thesis, these versions had only been initially validated against CMR-LGE in small populations, although with promising results[99]. Further, the Selvester QRS score was shown to be predictive of echocardiographic CRT-response[58], which was later corroborated[59]. Successful efforts were therefore made to automate the 2009 LBBB version of the Selvester QRS score (2009 LBSS)[100, 101], in parallel to its thorough evaluation against CMR-LGE.

Figure 14. The 2009 Selvester QRS score, adapted for conduction abnormalities.

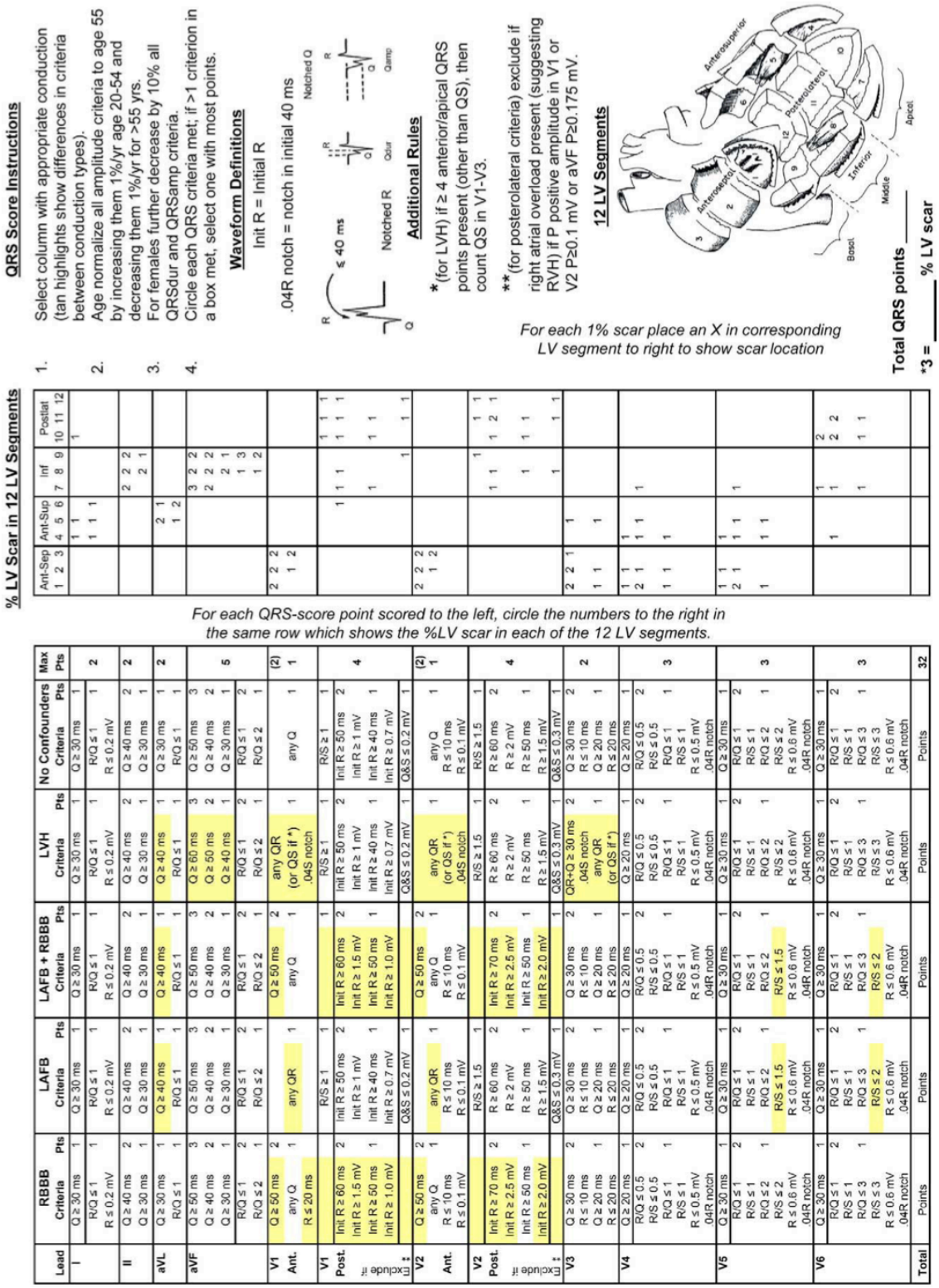

Figure 14. *The table to the left shows which set of QRS-morphology criteria is intended for which conduction type. Each score point translates into scar equivalent to roughly 3% of the LV mass, distributed within the LV according to the table in the middle. The right hand panel provides further instruction for the application of the Selvester QRS score. Criteria differing from the normal conduction Selvester QRS score are highlighted. Figure reproduced from Strauss, et al.,*[30] *with permission.*

Figure 15. The 2009 Selvester QRS score adapted for left bundle branch block

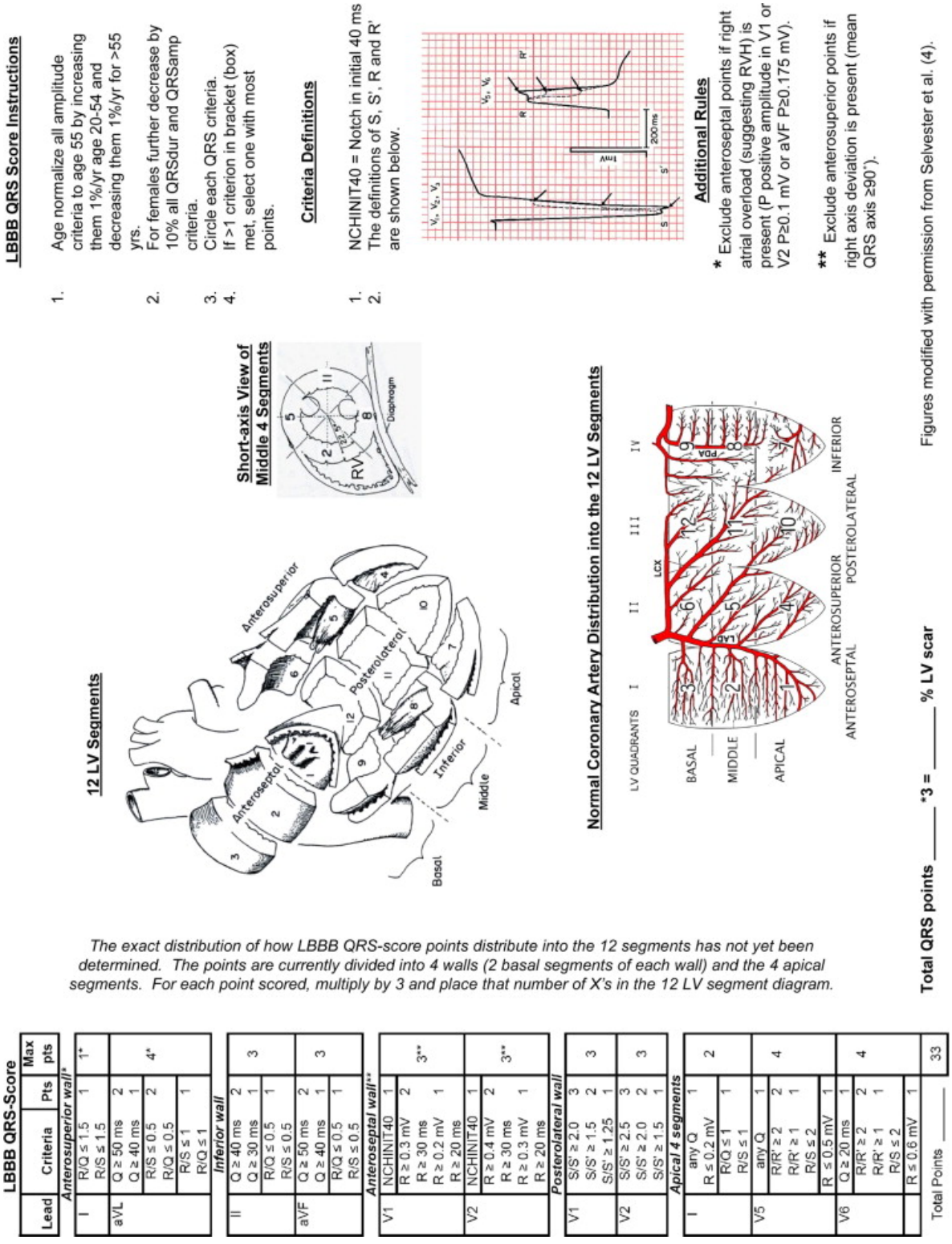

Figure 15. *The table to the left in the image shows the individual QRS-morphology criteria and their translation into points. Each point represents presence of scar roughly equivalent to 3% of the left ventricular mass. Further, each point is divided into one of five myocardial regions: four equiangular quadrants and the apex, as visualized in the middle section of the figure. The right panel contains instructions for the application of the score. Figure reproduced from Strauss, et al.,*[30] *with permission.*

2 AIM

The aim of this thesis was to investigate the ability of the 2009 Selvester QRS score to detect, quantify and localize myocardial scar in LBBB, RBBB, LAFB and RBBB+LAFB, with special emphasis on LBBB due to its importance in clinical decision-making regarding CRT. A secondary objective was to modify the Selvester QRS score to optimize electrocardiographic characterization of myocardial scar in the presence of LBBB.

The aims of each specific study were:

I) To determine the ability of the component criteria of the 2009 LBBB version of the Selvester QRS score (2009 LBSS) to localize myocardial scar into five myocardial wall regions.

II) To evaluate the performance of the 2009 Selvester QRS score to detect and quantify myocardial scar in four conduction abnormalitites: LBBB, RBBB, LAFB and the combination of RBBB+LAFB.

III) To measure the specificity of each of the component criteria of the 2009 LBSS in a population of patients with no scar verified by CMR.

IV) To determine the prognostic utility of Selvester QRS scoring in patients of various conduction types with or without CRT as an addition to ICD in the Multicenter Automated Defibrillator Implantation Trial – Cardiac Resynchronization therapy (MADIT-CRT) population.

V) To revise the 2009 LBSS through comparison of continuous ECG variables to CMR-identified myocardial scar presence and extent in a large multicenter dataset of patients with LBBB.

3 MATERIALS AND METHODS

3.1 STUDY POPULATIONS

The study population for study I consisted of the LBBB subgroup (n=39) of a cohort of 235 consecutive patients referred for ICD implantation at Johns Hopkins University Hospital, Baltimore, MD, USA[66], and did not overlap with the other studies in this thesis. Study IV was a substudy conducted in the large multicenter MADIT-CRT population[31], which did not overlap with the study populations from study I, II, III and V.

The study populations for study II, III and V partially overlapped and were composed of retrospectively identified patients that had LBBB, RBBB, LAFB or RBBB+LAFB determined by an ECG recorded close in time to a CMR scan at one of four centers: Karolinska University Hospital, Stockholm, Sweden; Skåne University Hospital, Lund, Sweden; Duke University Medical Center, Durham, NC, USA or University of Pittsburgh Medical Center, Pittsburgh, PA, USA. Study II was performed on consecutive patients at Duke University Medical Center who underwent CMR between January 2011 and August 2013 and had either one of the four conduction abnormalities LBBB, RBBB, LAFB or the combination of RBBB+LAFB by ECG. Study III included patients with no scar by CMR from Karolinska, Lund and Duke. Study V included all Karolinska patients from study III, the LBBB subgroup of the study population in study II and additional LBBB patients from all four centers mentioned above.

3.1.1 Study I

The study was conducted as a substudy of the LBBB subgroup of a prospectively enrolled cohort of patients referred for ICD with LVEF ≤35%. Enrollment took place at Johns Hopkins University Hospital during the period between November of 2003 and December 2010. Out of 235 patients in the cohort, 45 were identified as having LBBB by the Strauss

criteria described above. After two patients were excluded due to insufficient ECG quality, one for incomplete CMR coverage of the LV, and another three due to small scar the remaining 39 patients constituted the study population. Patients with small CMR scar were excluded in order to create clearly scar positive or scar negative groups in which to measure sensitivity and specificity of ECG criteria for scar in different areas of the LV.

Exclusion criteria during enrollment are described in full in a previous publication by the authors of the original prospective study[47] and were among others NYHA functional class IV, acute myocarditis, arrhythmic ICD indication, hypertrophic cardiomyopathy and congenital or storage heart disease. Furthermore, patients with creatinine-estimated clearance of < 30 ml per minute were excluded starting with patients enrolled in 2006. The year 2006 marked the discovery that such patients were at a small risk of developing nephrogenic systemic fibrosis following administration of gadolinium-based contrast agents[102].

All patients provided written informed consent to participate in the original prospective study[47]. The institutional review boards (IRB) at Duke University and Johns Hopkins University Hospital as well as the US Food and Drug administration (FDA) human research committee approved the study protocol for the substudy.

3.1.2 Study II

Study II was conducted using a retrospectively identified dataset consisting of all patients who underwent a clinically motivated CMR scan at Duke University Medical Center between August 2011 and January 2013 that had ECG evidence of either LBBB, RBBB, LAFB or the combination of RBBB+LAFB. Exclusion criteria were poor CMR image quality and poor quality ECG. The study protocol was approved by the Duke University IRB. Sample size, cohort characteristics and distribution according to conduction type is shown in table 2.

Table 2. Cohort characteristics of Study II population.

Characteristic	LBBB (n = 62)	RBBB (n = 51)	LAFB (n = 43)	RBBB + LAFB (n = 37)	Overall population (n = 193)
Age, mean ± SD (y)	63.0 ± 11.0	59.7 ± 16.8	61.7 ± 13.1	69.6 ± 12.7	63.1 ± 13.8
Sex, males, n (%)	30 (48)	37 (73)	34 (79)	26 (70)	127 (66)
HF medication, n (%)					
β-blocker	46 (74)	26 (51)	14 (33)	24 (65)	110 (57)
ACEi	23 (37)	10 (20)	12 (28)	18 (49)	63 (33)
ARB	10 (16)	11 (22)	3 (7)	4 (11)	28 (15)
Aldosterone antagonist	14 (23)	5 (10)	2 (5)	3 (8)	24 (12)
Cardiovascular health status and risk factors					
Active tobacco use, n (%)	3 (5)	1 (2)	5 (12)	6 (16)	15 (8)
CAD, n (%)	21 (34)	21 (41)	15 (35)	19 (51)	76 (39)
Hypertension, n (%)	37 (60)	26 (51)	58 (25)	29 (78)	117 (61)
Diabetes mellitus, n (%)	15 (24)	16 (31)	4 (9)	9 (24)	44 (23)
LVEF, mean ± SD (%)	43 ± 15	55 ± 12	52 ± 14	46 ± 19	49 ± 16
Ischemic cardiomyopathy, n (%)	21 (34)	22 (43)	12 (28)	15 (41)	70 (36)
Scar burden, mean ± SD (% LV mass)					
By CMR	2.3 ± 3.8	4.6 ± 10.2	4.0 ±8.2	9.0 ± 13.8	4.6 ± 9.4
By ECG	13.4 ± 9.7	10.0 ± 10.3	14.6 ± 8.8	20.0 ± 11.1	14.0 ± 10.4
Patients with 0% CMR scar, n (%)	37 (60)	25 (49)	24 (56)	10 (27)	96 (50)

Abbreviations: *HF*, heart failure; *ACEi*, angiotensin-converting enzyme inhibitor; *ARB*, angiotensin receptor blocker.

Table reproduced from Study II, with permission.

3.1.3 Study III

A total of 99 patients who had ECG evidence of LBBB by the Strauss criteria[19] and no myocardial scar were retrospectively identified from the clinical CMR databases at three centers: Duke University Medical Center, Karolinska University Hospital and Skåne University Hospital, Lund, Sweden. Inclusion criteria were ECG registration at the latest 30 days after CMR scan, acceptable quality CMR-LGE images to rule out myocardial scar and and sufficient quality ECG recording for application of the Selvester QRS score. The study population partially overlapped with that of study II, in that patients with LBBB and no scar were also included in study III. In addition, patients having undergone CMR at Karolinska University Hospital between 2003 and 2014 and at Lund from 2011 through 2014 were screened for participation. In order to identify patients who met inclusion criteria, the clinical CMR databases were compared against the clinical ECG databases to select patients with automatically detected LBBB. The resulting identified ECGs were then reviewed manually in order to include one ECG per patient that met Strauss criteria for LBBB that also had the highest quality and was closest in time to the CMR scan. The respective ethical committees at all three centers approved the study protocol. Furthermore, patients either provided written

informed consent or the requirement for written consent was retrospectively waived by the respective ethical committee or IRB.

3.1.4 Study IV

The fourth study was a substudy of the 1820 patients included in the prospective MADIT-CRT population[31], in which patients were randomized in a 2:3 fashion to either implantation of ICD alone or implantation of a combined CRT and ICD device (CRT-D). Inclusion criteria are described in detail in the original MADIT-CRT protocol[103] and were in summary: >21 years of age, ischemic (NYHA I-II) or non-ischemic (NYHA II only) cardiomyopathy and a QRS duration of >130 ms. Exclusion criteria included existing indication for either CRT or ICD according to criteria at enrollment, previously implanted CRT or ICD, coronary artery bypass graft (CABG) operation. A more detailed description of the study protocol is previously published[103]. This study population did not overlap with any of the other studies in this thesis.

3.1.5 Study V

Study V included patients with an available digital ECG and who had undergone a CMR scan for any reason at one of four centers: Pittsburgh University Medical Center, Duke University Medical Center, Karolinska University Hospital, Stockholm, Sweden and Skåne University Hospital, Lund. For three centers (Duke, Pittsburgh and Karolinska), clinical CMR databases were compared to the clinical ECG databases in order to screen for patients who met the Strauss criteria for LBBB and who had a good quality ECG recorded close in time to the CMR scan (<30 days, unless the ECG was recorded prior to CMR, in which case no time limit was required). The Lund patients were the LBBB subgroup from a separate ongoing prospective study that met the inclusion criteria of study V and had evidence of scar by CMR. Patients were excluded if either the ECG or CMR was of poor quality or if they had CMR

evidence of congenital heart disease, myectomy or infiltrative heart disease. The study population for study V included the Karolinska and Duke contingents of Study III and most of the patients with LBBB and myocardial scar from study II. Patients either provided written informed consent, or alternatively, the requirement for informed consent was waived retrospectively by the respective IRB or ethical committee. Approval was obtained from the IRB or ethical committee at each respective center.

3.2 ECG ACQUISITION AND ANALYSIS

Standard 12-lead ECGs were recorded under clinical conditions using clinical ECG machines from three different vendors, depending on center and time period, with the majority of the ECGs being recorded on a GE Marquette system (General Electric, Little Chalfront, UK). Other ECGs were recorded on either a Siemens system (Siemens, Erlangen, Germany) or a Philips system (Philips, Best, the Netherlands). Paper ECGs were printed out and deidentified for manual application of Selvester QRS scoring. For study V, digital ECGs were exported and digitally anonymized at each respective center.

3.2.1 Classification of conduction type

For studies concerning only LBBB or LBBB versus non-LBBB (studies I, III, IV and V) ECGs were classified as LBBB if they met Strauss criteria for LBBB[19]: ≥130 ms QRS duration (≥140 ms for men), rS or QS configuration in lead V1 and presence of mid-QRS notching or slurring in ≥ of leads I, aVL, V1, V2, V5 and V6. In study II, ECGs were classified into the following conduction types: LBBB, RBBB, LAFB, RBBB+LAFB or normal conduction in accordance with a previously published guide to the application of Selvester QRS scoring[84].

3.2.2 Application of the Selvester QRS score

Selvester QRS scoring was performed in accordance with a previously published guide[84] containing detailed definition of each waveform in the respective context of each of the individual component criteria listed in figures 14 and 15. Selvester scoring was performed by a single observer in studies I and IV. In study IV, a subset of ECGs flagged as difficult were also reviewed and adjudicated by a second observer. In studies II and III, Selvester QRS scoring was performed by two independent observers with disagreements being adjudicated in conference. For study V, continuous waveform measurements were obtained using a dedicated software, and these measurements were then used to calculate the Selvester QRS score.

3.2.3 Development of ECG analysis software

We developed a custom ECG analysis software in order to obtain detailed continuous ECG measurements. Software development was performed through an iterative process of user feedback and subsequent modifications, with all programming being performed by Xiaojuan Xia at Rochester University, New York, USA.

3.2.4 Continuous measurement on digital ECG recordings

The software allowed a stepwise measurement of both global and lead-by-lead QRS complex waveform metrics. The measurement process is summarized in figure 16. Global measurements were obtained by placement of fiducial markers on superimposed QRS median complexes of all 12 leads at QRS onset and offsets, as well as at the estimated start, peak and end of the LBBB notch required by the Strauss LBBB criteria. On a lead-by-lead basis, fiducial markers were placed whenever the signal crossed above or below the PQ-baseline, as well as at the peak of each waveform. Thus, the timing of the start, end and peak/nadir of Q, R, S, R', S', R'', S'' and so forth could be computed, as well as the maximum or minimum

amplitude of each waveform and the maximum and minimum amplitude of the overall QRS complex in each lead. In addition, the timing and amplitude of the start, end and peak/nadir of each notch and slur was recorded according to definitions in figure 16. As a rule, each slur or notch had to be judged to visually be of greater magnitude than background noise, which introduced a limited degree of subjectivity into the analysis.

Figure 16. Summary ECG measurement procedure in Study V

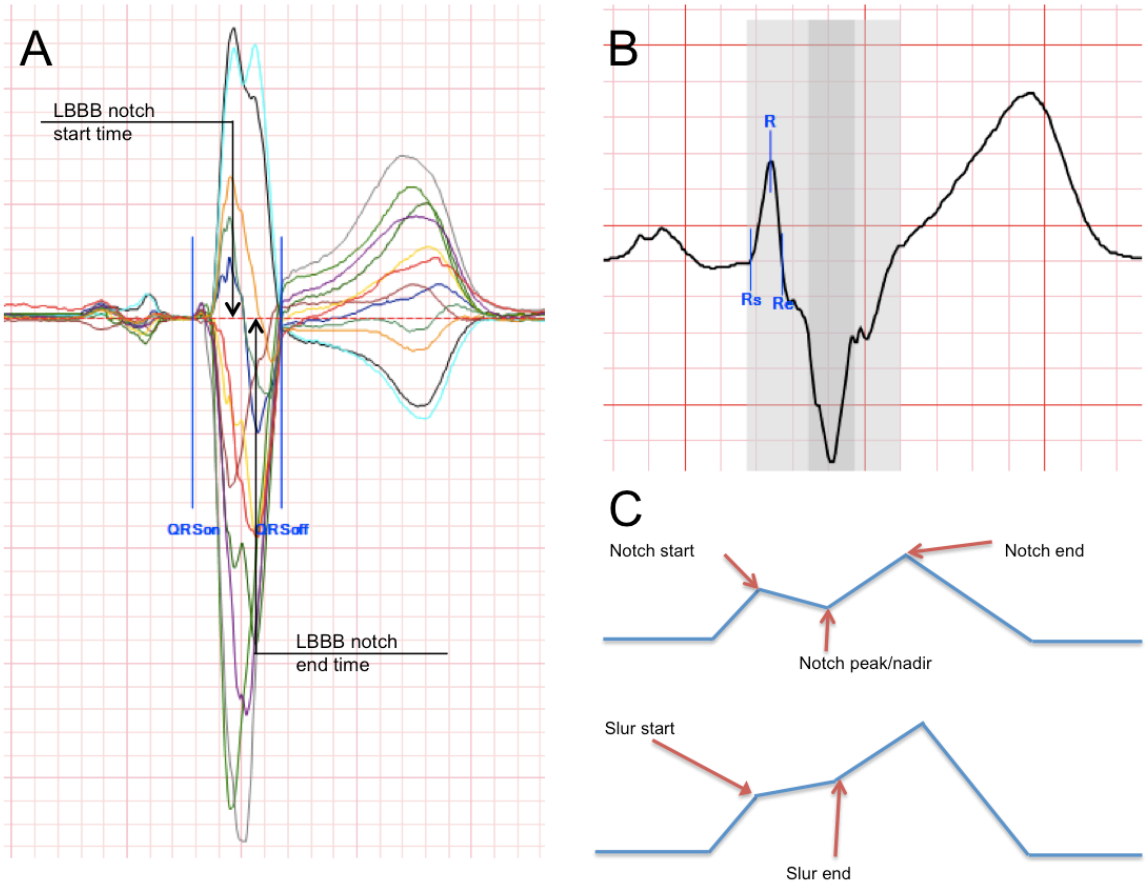

Figure 16. *This figure shows a summary of how continuous measurements were obtained from the digital ECGs in study V. First, fiducial markers were placed at the QRS on- and offset in a global view with median complexes of all superimposed (Panel A). Further, fiducial markers were placed at the visually estimated start and end of the mid-QRS notch or slur mandated by the Strauss criteria for LBBB[19]. Next, lead-by-lead waveform measurements were obtained as shown in Panel B by placing fiducial markers at the start, peak/nadir and end of each waveform. In addition, the timing and amplitude of the start and end of notches and slurs were recorded, as well as of the peak/nadir of notches in every lead. Panel C shows a schematic illustration of the working definitions of notch and slur measurements. Notches and slurs were disregarded if visually indistinguishable from baseline noise. Figure reproduced from Study V manuscript.*

3.3 CMR ACQUISITION AND ANALYSIS

The specifics of both scanners, coils, pulse sequences and contrast agents varied across centers and periods of time during which CMR scans were carried out. The CMR images were acquired at five centers: Johns Hopkins University Hospital (Study I), Duke University Medical Center (Studies II, III and V), Karolinska University Hospital (Studies III and V), Skåne University Hospital, Lund (Studies III and V) and University of Pittsburgh Medical Center (Study V). Both 1.5 T and 3.0 T scanners were used from multiple vendors. The 1.5 T scanners included: GE Signa CV/i (GE, Little Chalfront, UK); Philips Intera (Philips, Best, the Netherlands); Siemens Magnetom Espree, Aera and Avanto (Siemens, Erlangen, Germany). The 3.0 T scanners were: Philips Intera (Philips, Best, the Netherlands) and Siemens Verio (Siemens, Erlangen, Germany). Phased array cardiac receiver coils and ECG gating were used for all image acquisition. Specific contrast agents included: Gadoversetamide, Mallinkrodt Inc, St. Louis, MO, USA; gadoteridol, Prohance, Bracco Diagnostics, Monroe Township, NJ, USA; gadoteric acid, Guerbet, Gothia Medical AB, Billdal, Sweden and Gadoterate meglumine, Guerbet LLC, Bloomington, IN, USA). At all centers, viability imaging was performed using various LGE pulse sequences. These involved inversion recovery images with our without motion correction acquired typically 10-15 minutes after administration of 0.10-0.15 mmol per kg of bodyweight of one of the gadolinium-based contrast agents described above. Voxel dimensions varied with the field of view demanded by patient size, but were typically varied between 1.4^2-1.8^2 mm^2 in plane resolution, 6-8 mm slice thickness and a 0-4 mm interslice gap.

Cine images for study V were typically acquired using a steady-state free precession protocol prior to administration of contrast. Typical in plane resolution was close to 1.5x1.5 mm2 with a slice thickness and interslice gap of 6 mm and 4 mm, respectively. The typical

temporal resolution was between 25-40 frames per second, depending on protocol and heart rate. In general, 20-25 frames were recorded for one cardiac cycle.

3.3.1 CMR export and anonymization

For study V in which CMR images were exported and compiled into a dataset, CMR images were anonymized at each respective center. LGE images were exported for all patients. Cine images were inluded with matching slice positions whenever available. The local radiological information system (RIS) and Picture archiving and communications system (PACS) was accessed on-site at the four participating centers in study V. Next, images were exported to a local work station in standard Digital imaging and communications in medicine (DICOM) format. Images were then loaded into a locally installed version of the image analysis software Segment (Medviso, Lund, Sweden)[104, 105]. Subsequently, each patient was provided with a subject ID recorded into a local digital subject identifier key kept in computers within the local firewall of each respective center. Images were anonymized and exported as MATLAB formatted data (file extension ".mat"), after which anonymized images were stored and analyzed on a personal computer.

3.3.2 Analysis of late gadolinium enhancement images

Analysis of LGE images was performed differently for the different studies. In all studies, the presence of scar was visually determined and then confirmed in two consecutive or orthogonal slices. In study I, CMR scar was quantified as described previously[47] by manual delineation of visually determined scar borders and endo- and epicardial borders. The pixels within the area outlined as scar were divided into core scar (>50% of the maximal signal intensity within scar), gray zone scar[47] and healthy myocardium. Gray zone pixels were defined as having a signal intensity greater the peak signal intensity of a remote region of interest in healthy myocardium but lower signal intensity than core scar[47]. In study II, scar was visually quantified by dividing the LV into segments and then grading scar transmurality

in each segment as 0-4 with steps 1-4 corresponding to 25% transmurality incremental intervals. The subdivision model used was the 17-segment model shown in figure 17, endorsed by the AHA[106]. Next, the percentage of LV mass consisting of scar tissue was estimated by assuming that all 17 segments have equal mass and by approximating scar transmurality in each segment as the midpoint of the transmurality interval stipulated by each category. As an example, if a certain segment is thought to have a scar transmurality of 50-75%, it is assigned category 3. That segment is thus thought to contain scar mass equivalent to (50+75%)/2/17 = 3.7 % of the total LV mass. When every segment is summed up this way, an overall scar percentage of LV mass is yielded.

Figure 17. Polar plot of the AHA17 LV subdivision model

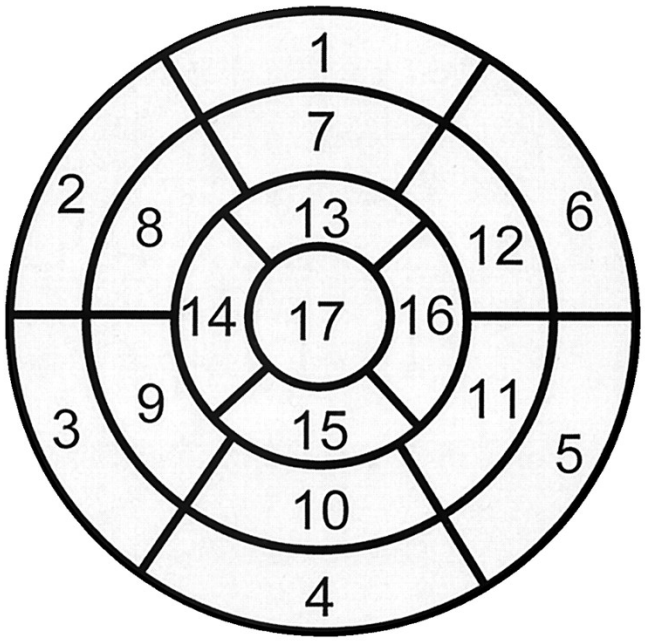

1. basal anterior
2. basal anteroseptal
3. basal inferoseptal
4. basal inferior
5. basal inferolateral
6. basal anterolateral
7. mid anterior
8. mid anteroseptal
9. mid inferoseptal
10. mid inferior
11. mid inferolateral
12. mid anterolateral
13. apical anterior
14. apical septal
15. apical inferior
16. apical lateral
17. apex

Figure 17. *The AHA 17-segment subdivision model displayed as a polar plot[106]. The left ventricle is depicted as a hemisphere viewed from below, with the middle circle representing the apex and concentric layers representing incrementally more basal myocardial wall regions. Figure reproduced from Cerqueira et al[106] with permission.*

For study V, presence of scar was visually determined by identification of LGE in either two consecutive short axis (SA) slices or in two orthogonal views. Scar was categorized as ischemic if areas with LGE were either subendocardial or transmural and approximately respected coronary artery distribution territories, as shown in figure 18. Patients with ambiguous scar etiology or borderline image quality were adjudicated by a second experienced observer. Scar was quantified using the appropriate semi-automatic algorithm in the software Segment (Medviso, Lund, Sweden)[104, 105], depending on whether LGE image inversion recovery type was either a phase sensitive (PSIR) or magnitude (MAGIR) reconstruction. The manual part of the scar quantification process in Segment involves delineation of endo- and epicardial borders for every slice covering the LV in a SA-stack as well as manual correction of erroneous scar detection due to artifacts.

Figure 18. The distribution of the AHA17 segments into coronary artery territories.

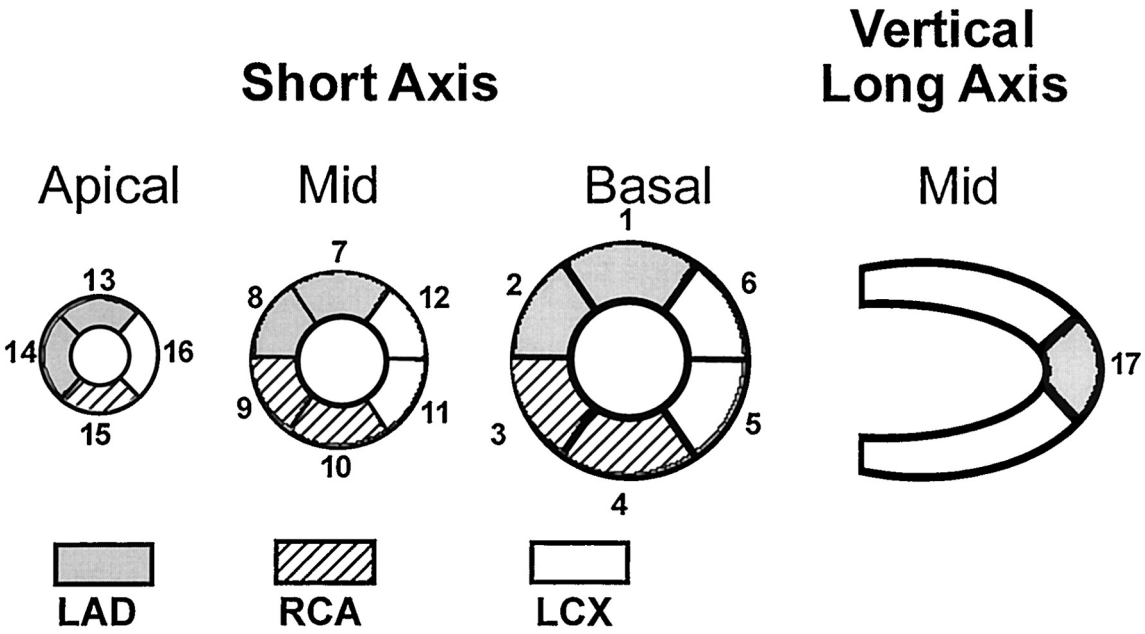

Figure 18. *This figure shows how the AHA17 segments are approximated into the coronary artery territories. Abbreviations: LAD - left anterior descending artery. RCA – Right coronary artery. LCX – left circumflex artery. Figure adapted from Cerqueira et al[106] with permission.*

All images were analyzed either by a single observer or by one observer performing delineation and second observer adjudicating the sometimes challenging delineation as well as performing manual corrections of automated scar quantification. The end output provided by the Segment software is global scar extent expressed as percentage of LV mass, as well as localized scar expressed as percent of each AHA17 segment, which is shown in figure 17.

3.3.3 Measurement of dimensions and function

Measurement of LVEF, LV mass (LVM) and end diastolic volume (EDV) were obtained from measurements performed on cine images either as part of clinical reports at each local center or as research measurements performed in Segment (Medviso, Lund, Sweden)[104, 105, 107, 108]. In Segment, the time frames representing end diastole (ED) and end systole (ES) were determined visually using both long axis (LA) images and a midventricular SA image. Next, endo- and epicardial borders were outlined in both ED and ES in the entire SA stack. LV function, expressed as LVEF, and LV dimensions, expressed as LVM and EDV, were then calculated in Segment based on known voxel dimensions and interslice gap. In addition, LVM and EDV were indexed (LVMI and EDVI) to body surface area (BSA) estimated from height and weight using the Dubois formula[109].

3.4 ECHOCARDIOGRAPHIC ANALYSIS

Echocardiographic analysis was performed at baseline and at 1-year follow-up in study IV at each respective center participating in the MADIT-CRT trial. Echocardiographic LVEF and EDV were computed using the Simpson model of discs as recommended by guidelines[110].

3.5 STATISTICAL ANALYSIS

Continuous background variables were reported as mean ± standard deviation (SD), with selected variables reported as median and range or interquartile range (IQR). In study V, normality of distribution was tested for using the Kolmogorov-Smirnov (K-S) test. Variables found to deviate significantly from normal in their distribution were reported in study V as median and IQR. Categorical variables were reported as absolute numbers and proportions.

Differences in means between two groups were tested for with the unpaired Students t-test. In cases with multiple groups, differences in means were tested for using analysis of variance (ANOVA) test. Correspondingly, differences in medians were tested for using Mann-Whitney U test or Kruskal-Wallis test, as appropriate. Differences in proportions were determined by Pearson's chi squared test. Ninety-five percent confidence intervals (95% CI) for means were estimated as the mean±1.96 times the standard error of means (SEM). For proportions, binomial 95% CIs were computed using the exact method. Cox proportional hazards were used to calculate hazard ratios (HR) for survival analysis. Linear correlations between continuous variables, such as myocardial scar estimated by both Selvester QRS scoring and CMR, were estimated using linear regression. In study II, agreement between continuous measurements was reported as intraclass correlation coefficient (ICC). Correlations between continuous predictor variables and binary outcomes were estimated using logistic regression. Performance of diagnostic tests was reported as specificity, sensitivity and area under the curve (AUC) derived from receiver operating characteristic (ROC) curves as well as intraclass correlation coefficient (ICC). Differences in AUCs were tested for using a previously described method[111]. In study I, a modified forward stepwise regression analysis approach was employed to identify the subset of 2009 LBSS criteria achieved best performance in diagnosing myocardial scar in a given myocardial wall region.

4 RESULTS AND DISCUSSION

Studies I-III concerned the performance of the 2009 LBSS versus CMR-LGE in detecting, quantifying and localizing myocardial scar. In study IV, the clinical utility of Selvester QRS scoring in predicting clinical benefit of CRT-D over ICD treatment only was investigated. Study V focused on revising and improving the 2009 LBSS.

4.1 LOCALIZATION OF MYOCARDIAL SCAR USING THE 2009 LBSS CRITERIA: STUDY I

Prior to the commencement of the study, high scar burden and lateral scar were both known to be associated with poor response to CRT[52, 54]. Simultaneously, a situation in HF care had evolved in which expensive CRT devices with potentially unwanted side effects were implanted in many patients with a non-response rate of approximately 30%[31]. Even though myocardial scar was thought to be a key factor in determining CRT appropriateness, performing a CMR scan on every candidate for CRT was not a widely adopted strategy due to restricted availability. Therefore, we addressed the prospect of using the inexpensive and widely available 12-lead ECG to screen for and localize myocardial scar as a simple strategy toward more targeted and individualized HF treatment.

The 2009 LBSS had not taken any empirical data into account during its construction but was purely a creation from theoretical model of conduction in LBBB (partially shown in figure 7, panel A). Still, each criterion was postulated to predict scar in one of five myocardial wall regions, as shown in figure 15. It thus appeared to be reasonable to expect a wide heterogeneity in diagnostic performance among the criteria. We therefore sought to identify the best performing combination of criteria to detect myocardial scar in each respective myocardial wall region. Because of a limited dataset (n=39 patients), study I likely suffered from overestimation of diagnostic performance from multiple testing. Therefore, study I had

the character of a pilot study indicating the likely maximum performance that could be expected at subsequent prospective evaluation. We chose to only focus on scar localization and not quantification in study I because a large portion of the same dataset had already been used to evaluate scar quantification.

In our hunt for the best performing subset of the 2009 LBSS criteria, we employed a modified forward stepwise regression approach in which we determined the highest possible sensitivity for a given level of specificity and subsequently sought to choose the highest combination of both as the best strategy. The performance of each constructed subset of the 2009 LBSS criteria is shown in figure 19.

Figure 19. Diagnostic performance of identified subsets of 2009 LBSS criteria shown in a receiver operating characteristic curve

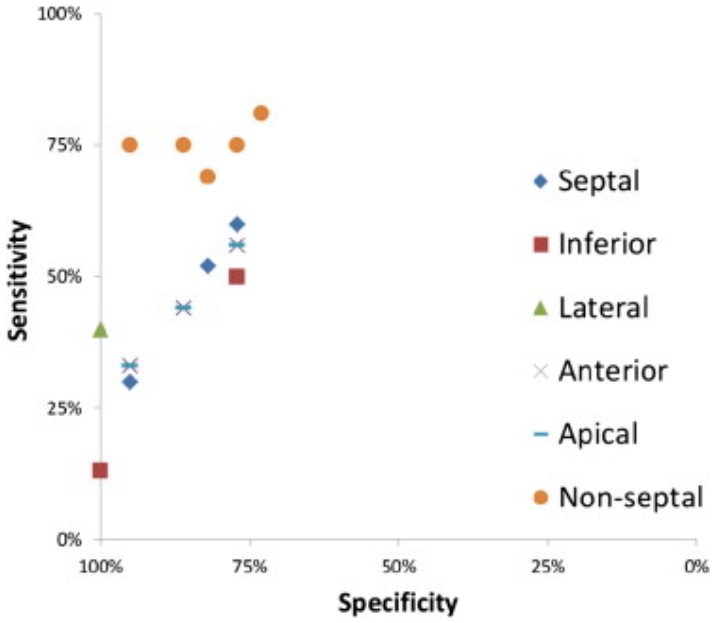

Figure 19. *The subsets of the 2009 LBSS criteria with optimal sensitivity for several predetermined levels of specificity to detect scar in given myocardial wall regions. The subset of criteria that was closest to the upper left corner was considered to have the optimal diagnostic performance for each respective myocardial wall region. The best subset of 2009 LBSS criteria for detection of non-septal scar achieved a specificity of 95% and sensitivity of 75 %. Figure adapted from Study I, with permission.*

In summary, the results of study I provided two insights:

1) The 2009 LBSS had limited performance in localizing myocardial scar into individual myocardial wall segments.
2) A set of criteria was found to detect presence of myocardial scar located anywhere but the septum in LV with reasonable performance, perhaps enough to be of clinical utility.

Although the non-septal set of criteria would have to be tested in an independent population and did not solely detect lateral scar, other studies had revealed that the CRT LV lead tips are implanted in all regions of the LV but the septum[112]. Furthermore, identified non-septal set of criteria was later found by an independent research group to be predictive of CRT response by echocardiography[60].

4.2 PERFORMANCE OF THE SELVESTER QRS SCORE IN A BROAD POPULATION IN SEVERAL CONDUCTION ABNORMALITIES: STUDY II

At the time of commencement of study II, the performance of the 2009 Selvester QRS score conduction abnormality adaptations had only been preliminarily evaluated against CMR-LGE in small and carefully selected datasets[99, 113, 114]. We therefore sought to evaluate the performance in detecting, quantifying and localizing myocardial scar in a wider population in four of the conduction types added in 2009: LBBB, RBBB, LAFB and the combination of RBBB+LAFB. At Duke, there was a high volume of patients undergoing CMR. Although patients with conduction abnormalities are likely overrepresented in clinical CMR databases in general, they constitute only a minority of patients. Between August 2011 and January 2013 there were 3962 patients who underwent both a CMR scan and an ECG at Duke University Medical Center. Out of these patients, there were 193 who had one of the included conduction abnormalities, a good quality ECG recording and a good quality CMR-LGE scan. They were distributed between conduction types according to table 2.

In summary, we found that the Selvester QRS score tended to both overestimate scar extent and presence. Diagnostic performance in terms of scar detection was modest with AUC ranging from 0.62-0.65 across the four conduction types. The correlation between the ECG and CMR estimated scar size was weak, with low ICC in all conduction types (table 3). The results inspired the hypothesis that some criteria were particularly non-specific. Also, an attempt at adjusting the Selvester QRS scores for the LAFB and RBBB+LAFB conduction types by discounting certain criteria thought to be non-specific yielded only slight improvement.

Table 3. Performance of the 2009 Selvester QRS score per conduction type (Study II)

	LBBB	RBBB	LAFB	LAFB (V_4-V_6 points excluded)	RBBB + LAFB	RBBB + LAFB (V_4-V_6 points excluded)
AUC (95% CI)	0.62 (0.48 to 0.76)	0.62 (0.49 to 0.79)	0.62 (0.44 to 0.81)	0.67 (0.52 to 0.83)	0.65 (0.46 to 0.84)	0.69 (0.50 to 0.87)
ICC (95% CI)	Negative/unestimable	0.45 (0.20 to 0.64)	0.19 (–0.12 to 0.46)	0.15 (–0.16 to 0.43)	0.25 (–0.08 to 0.53)	0.16 (–0.17 to 0.46)

Abbreviations: AUC – Area under the curve. ICC – intraclass correlation coefficient. LAFB – Left anterior fascicular block. LBBB – left bundle branch block. RBBB – Right bundle branch block. Table reproduced from Study II, with permission.

4.3 SPECIFICITIES OF THE 46 INDIVIDUAL CRITERIA COMPRISING THE 2009 LBSS: STUDY III

As a first step toward improving the ECG scar detection and quantification performance, we sought to investigate the specificities of individual criteria of the 2009 LBSS in order to determine if there were indeed highly non-specific criteria bogging down the performance of 2009 LBSS as a whole. Out of the several available conduction types, we chose to focus on LBBB for two main reasons. Firstly, LBBB was the clinically most important conduction abnormality because of the association with mechanical LV dyssynchrony. Secondly, the theoretically simple sequential activation pattern of the LV from right to left (shown in figure 7, panel A) was hypothesized to allow reasonably consistent ECG patterns and their readily detectable disrupting due to myocardial scar. We had also noted in previous studies that some criteria in the 2009 LBSS, such as location of the S' notch or slur[84] in the criteria for lateral

scar (listed in figure 15), were difficult to apply consistently. Therefore, we also measured interobserver variability on a per-criterion basis, rather than for the system as a whole, which had been previously reported to be excellent[115].

We did indeed find a great heterogeneity in specificity in the study population of 99 CMR-determined scar free patients, which ranged between 41-100 percent across the 46 criteria. We found somewhat lower interobserver agreement compared to a previous study by Strauss et al (full agreement in 39% and 60% of ECGs, respectively)[99], possibly because we only studied LBBB patients who may be more difficult to score than other conduction types. Moreover, we found varying interobserver agreement in the application of individual criteria, which ranged between 80-100 %. Specificity per criterion is shown in figure 20.

Figure 20. Specificity of the 46 QRS morphology criteria in the 2009 LBSS (Study III)

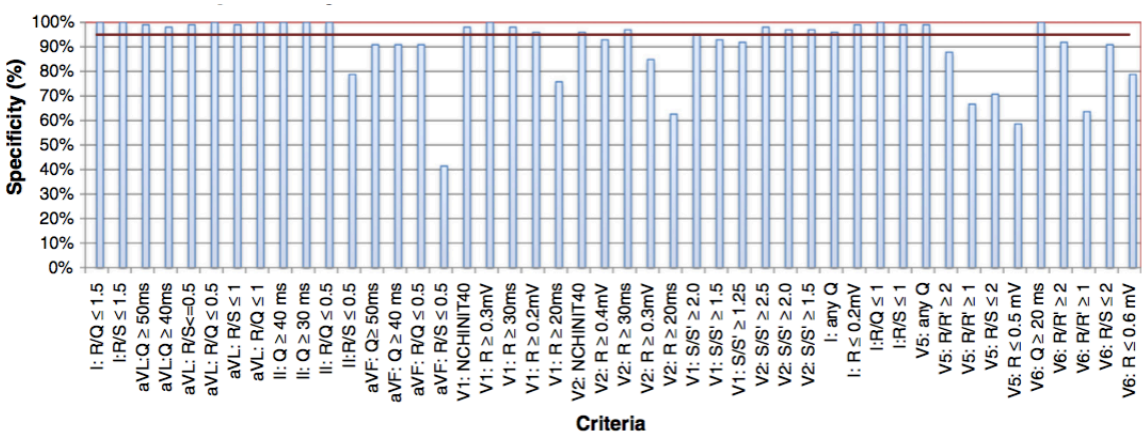

Figure 20. *The specificity of each och the individual criterion in the left bundle branch block adaptation of the 2009 Selvester QRS score. Figure reproduced from study III, with permission.*

4.4 USING THE 2009 LBSS TO PREDICT RESPONSE TO CRT: STUDY IV

Study IV commenced before the results of studies II and III were known. The Selvester QRS score in all conduction types had shown promising results in early validation versus CMR[99]. In study IV, paper ECG recordings from all 1820 patients in the MADIT-CRT database were

classified according to conduction type and then scored using previously published guide as a reference[84]. All ECG scoring was completed by Zak Loring and adjudication of difficult ECGs by David Strauss, both active at the US FDA at the time. A comprehensive analysis was performed in which the impact of Selvester QRS score on echocardiographic improvement and survival in both non-LBBB and LBBB subgroups was assessed. The ability of scar burden estimated by Selvester QRS scoring to predict heart failure event or death is summarized in figure 21.

In summary, we found that patients with higher Selvester QRS scores had increased mortality in the LBBB subgroups of both study arms. However, higher Selvester QRS score could not predict who would benefit from CRT. Still, high QRS score was predictive of less improvement post-CRT, but not faster deterioration in the absence of CRT. In addition, the effect of QRS score on echocardiographic parameters was significant but of a small effect magnitude. Linear regression indicated that a high QRS score of 10, hypothetically corresponding to roughly 30% LV scar, translating into 2.7 percentage points of lesser LVEF improvement. In light of the results from studies II and III, the results may have reflected the weak but still significant correlation between Selvester QRS score and myocardial scar. The results still highlight the importance of separating post-CRT prognosis from CRT efficacy. Previous findings have indicated that high scar burden is associated with poorer outcome after CRT, but only a randomized study could determine whether high scar burden is a merely a general marker of poor prognosis regardless of CRT. In the setting of HF with LBBB and high scar burden with a prognosis equivalent to many malignant diseases, it may be unethical to withhold a beneficial treatment only because that treatment would work even better in other patients. Indeed, a study comparing the effect of HF etiology on CRT benefit found that patients with ischemic etiology, who generally have higher scar burden, still benefit from CRT despite comparatively poor response in the CRT arm of the study[116].

Figure 21. Predictive power of Selvester QRS scoring in LBBB and non-LBBB subgroups of both study arms in study IV

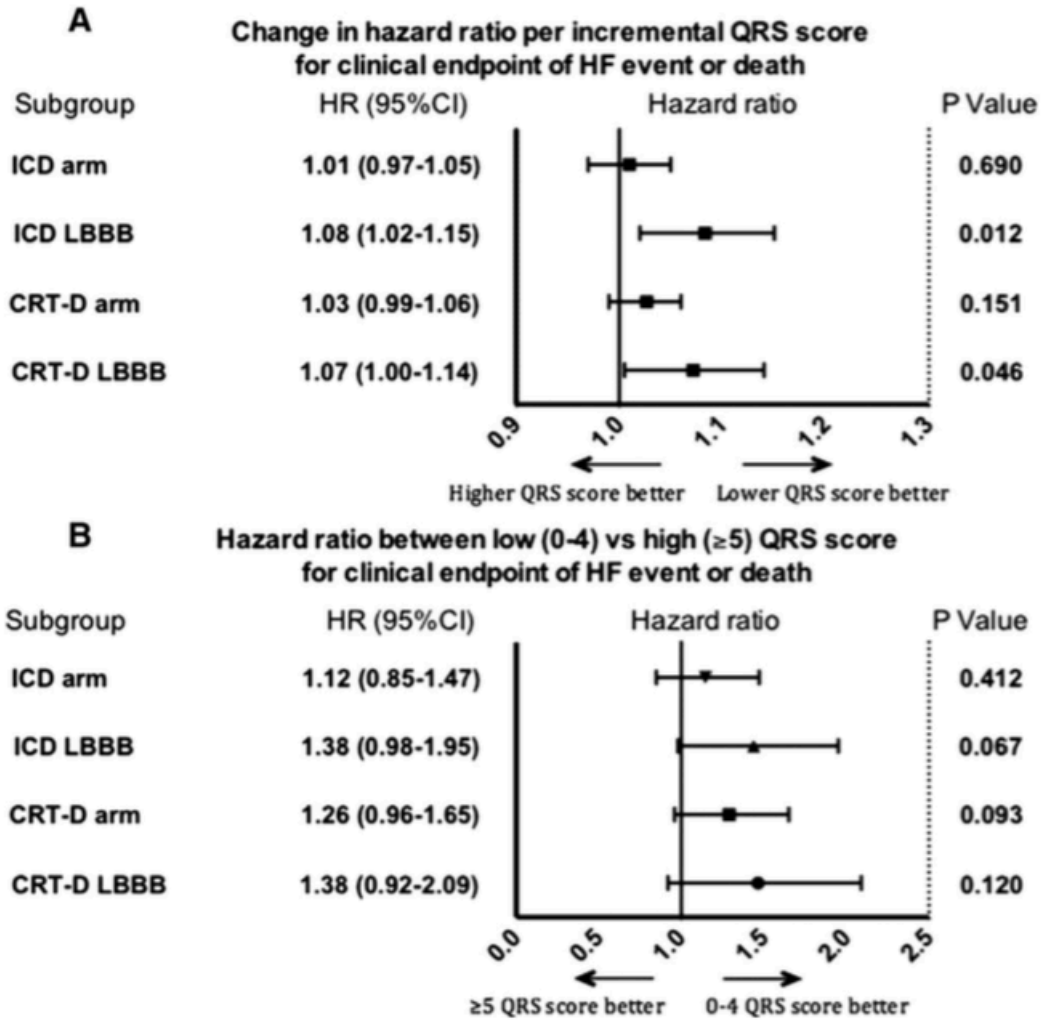

Figure 21. *Forest plots showing the effect of scar burden estimated by Selvester QRS scoring on risk of heart failure event or death, with QRS score as a continuous variable (panel A) and as a dichotomized variable (panel B). Each QRS score is thought to represent scar burden equivalent to 3% of the left ventricular mass. Abbreviations: CRT-D – Cardiac resynchronization therapy with defibrillator. ICD – Implantable cardioverter defibrillator. HF – Heart failure. Figure reproduced from Study IV, with permission.*

4.5 IMPROVED ECG SCAR CHARACTERIZATION IN LBBB: STUDY V

Study V was the largest and most complex study, in which we sought to assemble a large training set of patients with LBBB, known scar burden by CMR, and continuous ECG measurements to calibrate a new ECG scar screening tool using empirical data. The

theoretical groundwork had been laid down by the construction of the 2009 LBSS, shown in figure 15. Despite LBBB being relatively uncommon, clinical CMR databases had now grown so large since the general introduction of CMR-LGE imaging into clinical routine in the late 1990's and early 2000's that enough LBBB patients had undergone CMR. From the four participating centers, we were able to identify 325 patients with acceptable quality CMR and ECG measurements. We elected in study V to exclude patients who had more than 30 days in between the ECG acquisition and the CMR scan, unless there was no scar and the ECG was recorded first. The 2009 LBSS can be broken down into 21 continuous and 4 binary ECG variables. In addition to these, we elected to prospectively evaluate another 2 continuous and 16 binary ECG variables, assigned to specific myocardial wall regions. These additional ECG parameters were prospectively defined by three investigators in conference based on previous findings regarding the LBBB conduction pattern summarized in figure 7. In order to measure some of these variables, especially those involving notches and slurs, we deemed it necessary to create dedicated ECG analysis software as summarized in figure 16.

In analyzing the data, we first calculated the 2009 LBSS from the continuous ECG measurements for each patient and evaluated the performance. Results were largely consistent with those in study II, as both studies found an AUC to identify any scar of 0.62, with little improvement when various scar burden cutoffs were used so that only larger scars were counted as positive. Notably, there was no correlation between ECG and CMR scar in the 93 patients with ischemic scar. This absence of a correlation was surprising as dense focal ischemic scar would theoretically be easier to diagnose than more diffuse non-ischemic scar.

We attempted to develop an improved ECG scar screening and quantifying tool using several parallel approaches, all of which resulted in alternate systems that in turn were then evaluated with regards to ability to detect and quantify scar. Firstly, we attempted two modifications of the 2009 LBSS with a maintained overall structure. One alternate system was created in which all criteria were eliminated that did not meet a 95% specificity threshold according to

the results in study III. The other was based on tuning all thresholds of the continuous variables in the 2009 LBSS to exactly 95% specificity and then removing all binary criteria not meeting the specificty threshold. Neither of these approaches resulted in meaningful improvement.

Next, we used multivariate forward selection logistic regression to construct a model to detect presence of scar. This resulted in a significantly improved model compared to the 2009 LBSS (AUC 0.72 and 0.60, respectively, $p<0.006$). However, it should be acknowledged that the subgroup of patients with scar in the dataset was comprised of n=142 patients and there were 44 original candidate variables in the model. Thus the ratio of predictor variables to the rarest outcome, traditionally known as events per variable (EPV) was 3.3. In order to create generalizable models, an EPV of 10 is traditionally recommended. We still judged the approach beneficial enough to yield valuable results, partly as study of an estimated maximum performance of the ECG for detecting scar, and partly as a method for yielding a simple hypothesis that could more easily be tested prospectively.

Study V used multivariate forward selection linear regression to identify a model that could quantify myocardial scar burden. Unsurprisingly, an improvement was achieved in the training set compared to the 2009 LBSS although both methods had limited performance (r^2= 0.21 and 0.04, respectively, $p<0.001$).

We further evaluated all *a priori* defined ECG variables with regards to identifying scar in their assigned myocardial wall region with performance expressed as AUC (table 4). Notably, for the individual ECG parameter that best detected myocardial scar, maximum positive/maximum negative amplitude ratio in lead I, we found an AUC comparable to the multivariate logistic model described above (AUC 0.71 versus 0.72, $p=0.40$). Although both results run the risk of having been inflated due to overfitting, the performance is comparable in terms of combined sensitivity and specificity to traditional infarction diagnosis by

pathological Q-waves in patients with no conduction abnormality[83]. Furthermore, even small scar, prevalent in LBBB patients, has been shown to be a prognostically important[41, 45]. Thus, the 12-lead ECG likely does not contain the information necessary to quantify scar, but may be able to determine scar presence also in LBBB. The results can be evaluated in an independent population to determine the generalizability of the findings, which would not require extensive and time consuming CMR measurements of scar quantity as in study V.

Table 4. The ability of all evaluated ECG parameters to detect scar in their respective assigned myocardial wall regions (Study V)

ECG parameters, according to region and AUC	Area under the curve (95%CI)	ECG parameters, according to region and AUC	Area under the curve (95%CI)
Septal		***Lateral***	
Lead V2: R amplitude	0.57 (0.50-0.65)	QRS duration	0.67 (0.60-0.75)
Lead V1: R amplitude	0.56 (0.49-0.63)	Lead V1: S/S' amplitude ratio*	0.60 (0.53-0.68)
Lead V1: R duration	0.56 (0.49-0.63)	Lead V2: S/S' amplitude ratio*	0.59 (0.51-0.67)
Lead V2: R duration	0.54 (0.46-0.61)	Lead V2: Slur after global LBBB notch	0.56 (0.48-0.64)
Lead V1: Notch in initial 40 ms	0.53 (0.46-0.60)	Lead V3: Notch in last 3rd of QRS	0.56 (0.48-0.64)
Lead V2: Notch in initial 40 ms	0.52 (0.45-0.59)	Lead aVF: Notch in last 3rd of QRS	0.55 (0.47-0.63)
Inv QRS axis	0.51 (0.43-0.58)	Lead V4: Notch in last 3rd of QRS	0.54 (0.46-0.61)
Anterior		Lead III: Notch in last 3rd of QRS	0.53 (0.45-0.61)
Lead I: invMaxPos/MaxNeg amp	0.64 (0.57 -0.72)	Lead aVR: Notch in last 3rd of QRS	0.53 (0.46-0.61)
Lead aVL: invMaxPos/MaxNeg amp	0.64 (0.56-0.71)	Lead II: Notch in last 3rd of QRS	0.53 (0.45-0.61)
QRS duration	0.60 (0.52-0.68)	Lead V1: Notch in last 3rd of QRS	0.53 (0.45-0.61)
Lead aVL: Q duration	0.58 (0.50-0.67)	Lead V2: Notch in last 3rd of QRS	0.53 (0.45-0.61)
Inv QRS axis	0.54 (0.46-0.63)	Lead V5: Notch in last 3rd of QRS	0.52 (0.45-0.60)
Inferior		Lead V6: Notch in last 3rd of QRS	0.52 (0.45-0.60)
QRS duration	0.66 (0.59-0.73)	Lead aVL: Notch in last 3rd of QRS	0.52 (0.44-0.59)
Lead II: Q duration	0.54 (0.47-0.62)	Lead V1: Notch after LBBB notch	0.50 (0.43-0.58)
Lead II: invMaxPos/MaxNeg amp	0.54 (0.47-0.61)	Lead V2: Notch after LBBB notch	0.50 (0.42-0.58)
Lead aVF: Q duration	0.53 (0.46-0.61)	Lead V1: Slur after LBBB notch	0.50 (0.42-0.57)
Lead avF: invMaxPos/MaxNeg amp	0.49 (0.41-0.56)	Lead I: Notch in last 3rd of QRS	0.44 (0.47-0.52)
Apical			
Lead I: invMaxPos/MaxNeg amp	0.75 (0.69-0.81)		
QRS duration	0.67 (0.61-0.74)		
Lead V6: invMaxPos/MaxNeg amp	0.65 (0.59-0.71)		
Lead I: inv R amp	0.59 (0.53-0.66)		
Lead V5: invMaxPos/MaxNeg amp	0.58 (0.52-0.64)		
Lead V6: inv R amp	0.52 (0.45-0.59)		
Lead V5: inv R amp	0.52 (0.45-0.59)		
Lead V6: Q duration	0.52 (0.45-0.59)		
Lead I: Q duration	0.52 (0.45-0,59)		
Inv QRS axis	0.50 (0.43-0.57)		
Lead V5: Q duration	0.50 (0.43-0,57)		
Lead I: Q amp	0.48 (0.41-0.55)		
Lead V6: R/R' amp ratio*	0.46 (0.39-0.52)		
Lead V5: R/R' amp ratio*	0.43 (0.36-0.50)		

Abbreviations: Amp – Amplitude. AUC – Area Under the Curve. LBBB – Left Bundle Branch Block. InvMaxPos/MaxNeg amp – Inverted Maximum Positive Amplitude over Maximum Negative Amplitude Ratio. Table reproduced from study V manuscript.

5 CONCLUSIONS

Studies I-V collectively show that the 2009 Selvester QRS score for scar detection, quantification and localization in presence of conduction abnormalities typically overestimates scar presence and extent. Furthermore, the standard 12-lead ECG likely does not contain information needed to accurately localize and quantify myocardial scar in presence of LBBB. However, there may be simple ECG signs that can diagnose presence of myocardial scar with potentially comparable accuracy to traditional Q-waves in patients with normal conduction. These ECG patterns will have to be evaluated in an independent population, the work of which is being planned within the research group.

The specific conclusions for each paper were:

I. The 2009 LBSS criteria likely can convey some information about myocardial scar localization, but not enough to effectively rule out myocardial scar in a particular region in a clinical setting.

II. The conduction abnormality adaptations of the 2009 Selvester QRS score have limited agreement with CMR-LGE with regards to scar presence and extent, when evaluated in a broad population.

III. Several individual criteria of the 2009 LBSS have prohibitively low specificity.

IV. The 2009 Selvester QRS score is associated with increased risk of heart failure event or death regardless of CRT implantation.

V. The 12-lead ECG is not a suitable modality to accurately quantify myocardial scar in presence of LBBB. However, there may be simple patterns in the 12-lead ECG that may be able to detect myocardial scar presence.

6 ACKNOWLEDGEMENTS

I would like to thank the many people who have worked with me and supported me during the work with this thesis. I especially want to express my gratitude to…

My supervisors, **Martin Ugander**, **David G. Strauss**, **Andreas Sigfridsson** and **Kenneth Caidahl**, for teaching me the ropes of research, writing, presenting and teaching. Beyond the many hours of teaching directly and through example, **Martin Ugander** has always radiated an unending passion for science and has always made time when it mattered regardless of time of day. **Andreas Sigfridsson** has been an inexhaustible source of knowledge regarding any and all questions I have had about the mysteries of MRI physics. **Kenneth Caidahl** has taught me many lessons drawn from his long career in research. I would like to thank **David G. Strauss** for the important role he has played in getting me started in science and his substantial contributions to many of the papers in this thesis.

Brett D. Atwater for consistently being a joy to work with and for offering me so much support and so many opportunities and over the last few years.

Galen S. Wagner who kept challening and encouraging me to grow scientifically and personally from my first research experience even until the very last week of his life. After a long battle against leukemia, he sadly passed away shortly before the completion of this thesis on July 13th 2016. He will be missed dearly by myself and by the many scientists he has helped to succeed and flourish in research.

All **co-authors** of the papers in this thesis, not least **Zak Loring** and **Xiaojuan Xia** for their generosity with their time and energy, as well as **Igor Klem**, **Erik Schelbert** and **Henrik Engblom** with colleagues for graciously hosting me at their institutions.

All the wonderful people, who are too many to be named individually, at the **Department of Clinical Physiology** at Karolinska University Hospital for making all my time spent there so bright and rewarding during clinical work and research alike.

Magnus Lundin, **Jannike Nickander**, **Joakim Norderfeldt** and **Ingrid Berggren,** I did not know teaching ECG to medical students together could be that fun!

Everyone in the Karolinska CMR group, including those mentioned above as well as **Karen Holst, Peder Sörensson, Jenny Rasck, Sofie Olsson, Jonas Jenner, Eva Maret** and several others for their patience, laughter and warmth throughout my work with this thesis**.**

The medical students who I have had the priviliege of getting to know and work with during the time spent with this thesis, not least **Sofia Åkerlund** who is the first author of study III, and **Maren Maanja, Markus Hjorth** and **Jimmy Axelsson** who have all contributed in a major way to study V.

My fellow PhD students in the **Epi-mys** journal club, who have helped me to successfully navigate around unexpected obstacles during the completion of this thesis.

The **Tullus family** for their financial and continuing moral support.

Everyone in my wonderful **family,** who have all contributed in their own way, not least by providing the comfort of knowing that they are always there through ups and downs.

My girlfriend **Anna,** for all the help with the actual papers with everything from data analysis to proof reading, but more importantly for the neverending love and support.

7 REFERENCES

1. Horan LG. Manifest orientation: the theoretical link between the anatomy of the heart and the clinical electrocardiogram. *J Am Coll Cardiol*. 1987;9:1049-56.

2. Einthoven W. Le telecardiogramme. *Arch Int de Physiol*. 1906;4:*132-164*.

3. Henson JR. Descartes and the ECG lettering series. *J Hist Med Allied Sci*. 1971;26:181-6.

4. Fumagalli B. Unipolar value of standard limb leads; lead -VR and rational arrangement of limn leads. *Am Heart J*. 1954;48:204-23.

5. Koelsch S, Enge J and Jentschke S. Cardiac signatures of personality. *PLoS One*. 2012;7:e31441.

6. Jones MG, Anderson KM, Wilson PW, Kannel WB, Wagner NB and Wagner GS. Prognostic use of a QRS scoring system after hospital discharge for initial acute myocardial infarction in the Framingham cohort. *Am J Cardiol*. 1990;66:546-50.

7. Goldberger E. A simple, indifferent, electrocardiographic electrode of zero potential and a technique of obtaining augmented, unipolar, extremity leads. *American Heart Journal*. 1942;23:483-492.

8. H M. A method of analyzing the electrocardiogram. *Arch Int Med*. 1920;25:283-294.

9. Sur S, Han L and Tereshchenko LG. Comparison of sum absolute QRST integral, and temporal variability in depolarization and repolarization, measured by dynamic vectorcardiography approach, in healthy men and women. *PLoS One*. 2013;8:e57175.

10. Brightman MW and Reese TS. Junctions between intimately apposed cell membranes in the vertebrate brain. *J Cell Biol*. 1969;40:648-77.

11. Keith A and Flack M. The Form and Nature of the Muscular Connections between the Primary Divisions of the Vertebrate Heart. *J Anat Physiol*. 1907;41:172-89.

12. Kosowsky BD, Scherlag BJ and Damato AN. Re-evaluation of the atrial contribution to ventricular function: study using His bundle pacing. *Am J Cardiol*. 1968;21:518-24.

13. W E. Discovery of the pacemaker and heart conduction system in mammals. Fantasy and truth (translated from German). *Z Kardiol*. 1995;64:963-70.

14. George AL, Jr. Molecular and genetic basis of sudden cardiac death. *J Clin Invest*. 2013;123:75-83.

15. Durrer D, van Dam RT, Freud GE, Janse MJ, Meijler FL and Arzbaecher RC. Total excitation of the isolated human heart. *Circulation*. 1970;41:899-912.

16. Einthoven W. *(Nobel Lecture, 1925) " The string galvanometer and the measurement of the action currents of the heart" Nobel Lectures: Physiology or Medicine*. Amsterdam: Elsevier; 1965.

17. Elizari MV, Acunzo RS and Ferreiro M. Hemiblocks revisited. *Circulation*. 2007;115:1154-63.

18. Surawicz B, Childers R, Deal BJ, Gettes LS, Bailey JJ, Gorgels A, Hancock EW, Josephson M, Kligfield P, Kors JA, Macfarlane P, Mason JW, Mirvis DM, Okin P, Pahlm O, Rautaharju PM, van Herpen G, Wagner GS, Wellens H, American Heart Association Electrocardiography and Arrhythmias Committee CuoCC, Foundation ACoC and Society HR. AHA/ACCF/HRS recommendations for the standardization and interpretation of the electrocardiogram: part III: intraventricular conduction disturbances: a scientific statement from the American Heart Association Electrocardiography and Arrhythmias Committee, Council on Clinical Cardiology; the American College of Cardiology Foundation; and the Heart Rhythm Society. Endorsed by the International Society for Computerized Electrocardiology. *J Am Coll Cardiol*. 2009;53:976-81.

19. Strauss DG, Selvester RH and Wagner GS. Defining left bundle branch block in the era of cardiac resynchronization therapy. *Am J Cardiol*. 2011;107:927-34.

20. Auricchio A, Fantoni C, Regoli F, Carbucicchio C, Goette A, Geller C, Kloss M and Klein H. Characterization of left ventricular activation in patients with heart failure and left bundle-branch block. *Circulation*. 2004;109:1133-9.

21. Riera AR, Uchida AH, Schapachnik E, Dubner S, Zhang L, Filho CF, Ferreira C, Ferrara DE, de Luna AB and Moffa PJ. The history of left septal fascicular block: chronological considerations of a reality yet to be universally accepted. *Indian Pacing Electrophysiol J*. 2008;8:114-28.

22. Demoulin JC and Kulbertus HE. Histopathological examination of concept of left hemiblock. *Br Heart J*. 1972;34:807-14.

23. Fantoni C, Kawabata M, Massaro R, Regoli F, Raffa S, Arora V, Salerno-Uriarte JA, Klein HU and Auricchio A. Right and left ventricular activation sequence in patients with heart failure and right bundle branch block: a detailed analysis using three-dimensional non-fluoroscopic electroanatomic mapping system. *J Cardiovasc Electrophysiol*. 2005;16:112-9; discussion 120-1.

24. Jeong JH, Kim JH, Park YH, Han DC, Hwang KW, Lee DW, Oh JH, Song SG, Kim JS, Chun KJ, Hong TJ and Shin YW. Incidence of and risk factors for bundle branch block in adults older than 40 years. *Korean J Intern Med*. 2004;19:171-8.

25. LEV M. ANATOMIC BASIS FOR ATRIOVENTRICULAR BLOCK. *Am J Med*. 1964;37:742-8.

26. Massoullié G, Bordachar P, Ellenbogen KA, Souteyrand G, Jean F, Combaret N, Vorilhon C, Clerfond G, Farhat M, Ritter P, Citron B, Lusson JR, Motreff P, Ploux S and Eschalier R. New-Onset Left Bundle Branch Block Induced by Transcutaneous Aortic Valve Implantation. *Am J Cardiol*. 2016;117:867-73.

27. Strauss DG, Loring Z, Selvester RH, Gerstenblith G, Tomaselli G, Weiss RG, Wagner GS and Wu KC. Right, but not left, bundle branch block is associated with large anteroseptal scar. *J Am Coll Cardiol*. 2013;62:959-67.

28. Witt CM, Wu G, Yang D, Hodge DO, Roger VL and Cha YM. Outcomes With Left Bundle Branch Block and Mildly to Moderately Reduced Left Ventricular Function. *JACC Heart Fail*. 2016.

29. Francia P, Balla C, Paneni F and Volpe M. Left bundle-branch block--pathophysiology, prognosis, and clinical management. *Clin Cardiol*. 2007;30:110-5.

30. Strauss DG and Selvester RH. The QRS complex--a biomarker that "images" the heart: QRS scores to quantify myocardial scar in the presence of normal and abnormal ventricular conduction. *J Electrocardiol*. 2009;42:85-96.

31. Moss AJ, Hall WJ, Cannom DS, Klein H, Brown MW, Daubert JP, Estes NA, 3rd, Foster E, Greenberg H, Higgins SL, Pfeffer MA, Solomon SD, Wilber D, Zareba W and Investigators M-CT. Cardiac-resynchronization therapy for the prevention of heart-failure events. *N Engl J Med*. 2009;361:1329-38.

32. Xiang L, Zhong A, You T, Chen J, Xu W and Shi M. Prognostic Significance of Right Bundle Branch Block for Patients with Acute Myocardial Infarction: A Systematic Review and Meta-Analysis. *Med Sci Monit*. 2016;22:998-1004.

33. Xiong Y, Wang L, Liu W, Hankey GJ, Xu B and Wang S. The Prognostic Significance of Right Bundle Branch Block: A Meta-analysis of Prospective Cohort Studies. *Clin Cardiol*. 2015;38:604-13.

34. Mandyam MC, Soliman EZ, Heckbert SR, Vittinghoff E and Marcus GM. Long-term outcomes of left anterior fascicular block in the absence of overt cardiovascular disease. *JAMA*. 2013;309:1587-8.

35. Yancy CW, Jessup M, Bozkurt B, Butler J, Casey DE, Drazner MH, Fonarow GC, Geraci SA, Horwich T, Januzzi JL, Johnson MR, Kasper EK, Levy WC, Masoudi FA, McBride PE, McMurray JJ, Mitchell JE, Peterson PN, Riegel B, Sam F, Stevenson LW, Tang WH, Tsai EJ, Wilkoff BL, Foundation ACoC and Guidelines AHATFoP. 2013 ACCF/AHA guideline for the management of heart failure: a report of the American College of Cardiology Foundation/American Heart Association Task Force on Practice Guidelines. *J Am Coll Cardiol*. 2013;62:e147-239.

36. Mastandrea P. The diagnostic utility of brain natriuretic peptide in heart failure patients presenting with acute dyspnea: a meta-analysis. *Clin Chem Lab Med*. 2013;51:1155-65.

37. *Criteria Committee NYHA, Inc. Diseases of the Heart and Blood Vessels. Nomenclature and Criteria for diagnosis, 6th edition. Criteria Committee, New York Heart Association , Inc. Diseases of the Heart and Blood Vessels. Nomenclature and Criteria for diagnosis, 6th edition Boston, Little, Brown and Co. 1964, p 114*: *Boston, Little, Brown and Co.*; 1964.

38. Drazner MH. The progression of hypertensive heart disease. *Circulation*. 2011;123:327-34.

39. Mahrholdt H, Wagner A, Judd RM, Sechtem U and Kim RJ. Delayed enhancement cardiovascular magnetic resonance assessment of non-ischaemic cardiomyopathies. *Eur Heart J*. 2005;26:1461-74.

40. Radu RI, Bold A, Pop OT, Mălăescu DG, Gheorghişor I and Mogoantă L. Histological and immunohistochemical changes of the myocardium in dilated cardiomyopathy. *Rom J Morphol Embryol*. 2012;53:269-75.

41. Neilan TG, Coelho-Filho OR, Danik SB, Shah RV, Dodson JA, Verdini DJ, Tokuda M, Daly CA, Tedrow UB, Stevenson WG, Jerosch-Herold M, Ghoshhajra BB and Kwong RY. CMR quantification of myocardial scar provides additive prognostic information in nonischemic cardiomyopathy. *JACC Cardiovasc Imaging*. 2013;6:944-54.

42. Kwong RY and Korlakunta H. Diagnostic and prognostic value of cardiac magnetic resonance imaging in assessing myocardial viability. *Top Magn Reson Imaging*. 2008;19:15-24.

43. Kwong RY, Chan AK, Brown KA, Chan CW, Reynolds HG, Tsang S and Davis RB. Impact of unrecognized myocardial scar detected by cardiac magnetic resonance imaging on event-free survival in patients presenting with signs or symptoms of coronary artery disease. *Circulation*. 2006;113:2733-43.

44. Neilan TG, Shah RV, Abbasi SA, Farhad H, Groarke JD, Dodson JA, Coelho-Filho O, McMullan CJ, Heydari B, Michaud GF, John RM, van der Geest R, Steigner ML, Blankstein R, Jerosch-Herold M and Kwong RY. The incidence, pattern, and prognostic value of left ventricular myocardial scar by late gadolinium enhancement in patients with atrial fibrillation. *J Am Coll Cardiol*. 2013;62:2205-14.

45. Wu KC, Weiss RG, Thiemann DR, Kitagawa K, Schmidt A, Dalal D, Lai S, Bluemke DA, Gerstenblith G, Marban E, Tomaselli GF and Lima JA. Late gadolinium enhancement by cardiovascular magnetic resonance heralds an adverse prognosis in nonischemic cardiomyopathy. *J Am Coll Cardiol*. 2008;51:2414-21.

46. O'Gara PT, Kushner FG, Ascheim DD, Casey DE, Chung MK, de Lemos JA, Ettinger SM, Fang JC, Fesmire FM, Franklin BA, Granger CB, Krumholz HM, Linderbaum JA, Morrow DA, Newby LK, Ornato JP, Ou N, Radford MJ, Tamis-Holland JE, Tommaso CL, Tracy CM, Woo YJ, Zhao DX, Foundation ACoC, Guidelines AHATFoP, Physicians ACoE and Interventions SfCAa. 2013 ACCF/AHA guideline for the management of ST-elevation myocardial infarction: executive summary: a report of the American College of Cardiology Foundation/American Heart Association Task Force on Practice Guidelines: developed in collaboration with the American College of Emergency Physicians and Society for Cardiovascular Angiography and Interventions. *Catheter Cardiovasc Interv*. 2013;82:E1-27.

47. Schmidt A, Azevedo CF, Cheng A, Gupta SN, Bluemke DA, Foo TK, Gerstenblith G, Weiss RG, Marban E, Tomaselli GF, Lima JA and Wu KC. Infarct tissue heterogeneity by magnetic resonance imaging identifies enhanced cardiac arrhythmia susceptibility in patients with left ventricular dysfunction. *Circulation*. 2007;115:2006-14.

48. Leyva F, Foley PW, Chalil S, Ratib K, Smith RE, Prinzen F and Auricchio A. Cardiac resynchronization therapy guided by late gadolinium-enhancement cardiovascular magnetic resonance. *J Cardiovasc Magn Reson*. 2011;13:29.

49. Bilchick KC, Dimaano V, Wu KC, Helm RH, Weiss RG, Lima JA, Berger RD, Tomaselli GF, Bluemke DA, Halperin HR, Abraham T, Kass DA and Lardo AC. Cardiac magnetic resonance assessment of dyssynchrony and myocardial scar predicts function class improvement following cardiac resynchronization therapy. *JACC Cardiovasc Imaging*. 2008;1:561-8.

50. Ugander M, Ekmehag B and Arheden H. The relationship between left ventricular ejection fraction and infarct size assessed by MRI. *Scand Cardiovasc J*. 2008;42:137-45.

51. Iles L, Pfluger H, Lefkovits L, Butler MJ, Kistler PM, Kaye DM and Taylor AJ. Myocardial fibrosis predicts appropriate device therapy in patients with implantable cardioverter-defibrillators for primary prevention of sudden cardiac death. *J Am Coll Cardiol*. 2011;57:821-8.

52. Bleeker GB, Kaandorp TA, Lamb HJ, Boersma E, Steendijk P, de Roos A, van der Wall EE, Schalij MJ and Bax JJ. Effect of posterolateral scar tissue on clinical and echocardiographic improvement after cardiac resynchronization therapy. *Circulation*. 2006;113:969-76.

53. Chalil S, Foley PW, Muyhaldeen SA, Patel KC, Yousef ZR, Smith RE, Frenneaux MP and Leyva F. Late gadolinium enhancement-cardiovascular magnetic resonance as a predictor of response to cardiac resynchronization therapy in patients with ischaemic cardiomyopathy. *Europace*. 2007;9:1031-7. Epub 2007 Oct 12.

54. Leyva F. Cardiac resynchronization therapy guided by cardiovascular magnetic resonance. *J Cardiovasc Magn Reson*. 2010;12:64.:10.1186/1532-429X-12-64.

55. Schelbert EB, Cao JJ, Sigurdsson S, Aspelund T, Kellman P, Aletras AH, Dyke CK, Thorgeirsson G, Eiriksdottir G, Launer LJ, Gudnason V, Harris TB and Arai AE. Prevalence and prognosis of unrecognized myocardial infarction determined by cardiac magnetic resonance in older adults. *JAMA*. 2012;308:890-6.

56. Turkbey EB, Nacif MS, Guo M, McClelland RL, Teixeira PB, Bild DE, Barr RG, Shea S, Post W, Burke G, Budoff MJ, Folsom AR, Liu CY, Lima JA and Bluemke DA. Prevalence and Correlates of Myocardial Scar in a US Cohort. *JAMA*. 2015;314:1945-54.

57. Adelstein EC and Saba S. Scar burden by myocardial perfusion imaging predicts echocardiographic response to cardiac resynchronization therapy in ischemic cardiomyopathy. *Am Heart J*. 2007;153:105-12.

58. Sweeney MO, van Bommel RJ, Schalij MJ, Borleffs CJ, Hellkamp AS and Bax JJ. Analysis of ventricular activation using surface electrocardiography to predict left ventricular reverse volumetric remodeling during cardiac resynchronization therapy. *Circulation*. 2010;121:626-34.

59. Atwater BD, Babatunde A, Swan C, Wieslander B, Andresen A, Rabineau D, Tomfohr J, Wagner G, Jackson KP and Daubert JP. ECG myocardial scar quantification predicts reverse left ventricular remodeling and survival after cardiac resynchronization therapy implantation: A retrospective pilot study. *J Electrocardiol*. 2015;48:565-70.

60. Bani R, Checchi L, Cartei S, Pieragnoli P, Ricciardi G, Paoletti Perini A, Padeletti M, Michelotti F, Michelucci A, Mascioli G and Padeletti L. Simplified Selvester Score: a practical electrocardiographic instrument to predict response to CRT. *J Electrocardiol*. 2015;48:62-8.

61. Varma N. Left ventricular electrical activation during right ventricular pacing in heart failure patients with LBBB: visualization by electrocardiographic imaging and implications for cardiac resynchronization therapy. *J Electrocardiol*. 2015;48:53-61.

62. Bakker PF, Meijburg HW, de Vries JW, Mower MM, Thomas AC, Hull ML, Robles De Medina EO and Bredée JJ. Biventricular pacing in end-stage heart failure improves functional capacity and left ventricular function. *J Interv Card Electrophysiol*. 2000;4:395-404.

63. El-Sherif N, Amay-Y-Leon F, Schonfield C, Scherlag BJ, Rosen K, Lazzara R and Wyndham C. Normalization of bundle branch block patterns by distal His bundle pacing. Clinical and experimental evidence of longitudinal dissociation in the pathologic his bundle. *Circulation*. 1978;57:473-83.

64. Lee MA, Dae MW, Langberg JJ, Griffin JC, Chin MC, Finkbeiner WE, O'Connell JW, Botvinick E, Scheinman MM and Rosenqvist M. Effects of long-term right ventricular apical pacing on left ventricular perfusion, innervation, function and histology. *J Am Coll Cardiol*. 1994;24:225-32.

65. Padeletti L, Pieragnoli P, Ricciardi G, Innocenti L, Checchi L, Padeletti M, Michelucci A, Picariello F and Valsecchi S. Simultaneous His Bundle and Left Ventricular Pacing for Optimal Cardiac Resynchronization Therapy Delivery: Acute Hemodynamic Assessment by Pressure-Volume Loops. *Circ Arrhythm Electrophysiol*. 2016;9.

66. Wu KC, Gerstenblith G, Guallar E, Marine JE, Dalal D, Cheng A, Marban E, Lima JA, Tomaselli GF and Weiss RG. Combined cardiac magnetic resonance imaging and C-reactive protein levels identify a cohort at low risk for defibrillator firings and death. *Circ Cardiovasc Imaging*. 2012;5:178-86.

67. Rademakers LM, van Kerckhoven R, van Deursen CJ, Strik M, van Hunnik A, Kuiper M, Lampert A, Klersy C, Leyva F, Auricchio A, Maessen JG and Prinzen FW. Myocardial infarction does not preclude electrical and hemodynamic benefits of cardiac resynchronization therapy in dyssynchronous canine hearts. *Circ Arrhythm Electrophysiol*. 2010;3:361-8.

68. Kim RJ, Fieno DS, Parrish TB, Harris K, Chen EL, Simonetti O, Bundy J, Finn JP, Klocke FJ and Judd RM. Relationship of MRI delayed contrast enhancement to irreversible injury, infarct age, and contractile function. *Circulation*. 1999;100:1992-2002.

69. Kim RJ, Shah DJ and Judd RM. How we perform delayed enhancement imaging. *J Cardiovasc Magn Reson*. 2003;5:505-14.

70. Anderson KR, Sutton MG and Lie JT. Histopathological types of cardiac fibrosis in myocardial disease. *J Pathol*. 1979;128:79-85.

71. Rösner A, Avenarius D, Malm S, Iqbal A, Bijnens B and Schirmer H. Severe regional myocardial dysfunction by stress echocardiography does not predict the presence of transmural scarring in chronic coronary artery disease. *Eur Heart J Cardiovasc Imaging*. 2015;16:1074-81.

72. Gerber BL, Belge B, Legros GJ, Lim P, Poncelet A, Pasquet A, Gisellu G, Coche E and Vanoverschelde JL. Characterization of acute and chronic myocardial infarcts by multidetector computed tomography: comparison with contrast-enhanced magnetic resonance. *Circulation*. 2006;113:823-33. Epub 2006 Feb 6.

73. Baks T, Cademartiri F, Moelker AD, Weustink AC, van Geuns RJ, Mollet NR, Krestin GP, Duncker DJ and de Feyter PJ. Multislice computed tomography and magnetic resonance imaging for the assessment of reperfused acute myocardial infarction. *J Am Coll Cardiol*. 2006;48:144-52. Epub 2006 Jun 9.

74. Lardo AC, Cordeiro MA, Silva C, Amado LC, George RT, Saliaris AP, Schuleri KH, Fernandes VR, Zviman M, Nazarian S, Halperin HR, Wu KC, Hare JM and Lima JA. Contrast-enhanced multidetector computed tomography viability imaging after myocardial infarction: characterization of myocyte death, microvascular obstruction, and chronic scar. *Circulation*. 2006;113:394-404.

75. Mahnken AH, Koos R, Katoh M, Wildberger JE, Spuentrup E, Buecker A, Gunther RW and Kuhl HP. Assessment of myocardial viability in reperfused acute myocardial infarction using 16-slice computed tomography in comparison to magnetic resonance imaging. *J Am Coll Cardiol*. 2005;45:2042-7.

76. Kakimoto Y, Tsuruyama T, Miyao M, Abiru H, Sumiyoshi S, Kotani H, Haga H and Tamaki K. The effectiveness and limitations of triphenyltetrazolium chloride to detect acute myocardial infarction at forensic autopsy. *Am J Forensic Med Pathol*. 2013;34:242-7.

77. Prineas R, Richard SC and Zhang Z-m. *The Minnesota Code Manual of Electrocardiographical findings*. London: Springer; 2010.

78. Rautaharju PM, Surawicz B, Gettes LS, Bailey JJ, Childers R, Deal BJ, Gorgels A, Hancock EW, Josephson M, Kligfield P, Kors JA, Macfarlane P, Mason JW, Mirvis DM, Okin P, Pahlm O, van Herpen G, Wagner GS, Wellens H, American Heart Association Electrocardiography and Arrhythmias Committee CuoCC, Foundation ACoC and Society HR. AHA/ACCF/HRS recommendations for the standardization and interpretation of the electrocardiogram: part IV: the ST segment, T and U waves, and the QT interval: a scientific statement from the American Heart Association Electrocardiography and Arrhythmias Committee, Council on Clinical Cardiology; the American College of Cardiology Foundation; and the Heart Rhythm Society. Endorsed by the International Society for Computerized Electrocardiology. *J Am Coll Cardiol*. 2009;53:982-91.

79. Hancock EW, Deal BJ, Mirvis DM, Okin P, Kligfield P, Gettes LS, Bailey JJ, Childers R, Gorgels A, Josephson M, Kors JA, Macfarlane P, Mason JW, Pahlm O, Rautaharju PM, Surawicz B, van Herpen G, Wagner GS, Wellens H, American Heart Association Electrocardiography and Arrhythmias Committee CuoCC, Foundation ACoC and Society HR. AHA/ACCF/HRS recommendations for the standardization and interpretation of the electrocardiogram: part V: electrocardiogram changes associated with

cardiac chamber hypertrophy: a scientific statement from the American Heart Association Electrocardiography and Arrhythmias Committee, Council on Clinical Cardiology; the American College of Cardiology Foundation; and the Heart Rhythm Society. Endorsed by the International Society for Computerized Electrocardiology. *J Am Coll Cardiol*. 2009;53:992-1002.

80. Wagner GS, Macfarlane P, Wellens H, Josephson M, Gorgels A, Mirvis DM, Pahlm O, Surawicz B, Kligfield P, Childers R, Gettes LS, Bailey JJ, Deal BJ, Hancock EW, Kors JA, Mason JW, Okin P, Rautaharju PM, van Herpen G, American Heart Association Electrocardiography and Arrhythmias Committee CuoCC, Foundation ACoC and Society HR. AHA/ACCF/HRS recommendations for the standardization and interpretation of the electrocardiogram: part VI: acute ischemia/infarction: a scientific statement from the American Heart Association Electrocardiography and Arrhythmias Committee, Council on Clinical Cardiology; the American College of Cardiology Foundation; and the Heart Rhythm Society. Endorsed by the International Society for Computerized Electrocardiology. *J Am Coll Cardiol*. 2009;53:1003-11.

81. Kligfield P, Gettes LS, Bailey JJ, Childers R, Deal BJ, Hancock EW, van Herpen G, Kors JA, Macfarlane P, Mirvis DM, Pahlm O, Rautaharju P, Wagner GS, American Heart Association Electrocardiography and Arrhythmias Committee CuoCC, Foundation ACoC and Society HR. Recommendations for the standardization and interpretation of the electrocardiogram. Part I: The electrocardiogram and its technology. A scientific statement from the American Heart Association Electrocardiography and Arrhythmias Committee, Council on Clinical Cardiology; the American College of Cardiology Foundation; and the Heart Rhythm Society. *Heart Rhythm*. 2007;4:394-412.

82. Mason JW, Hancock EW, Gettes LS, American Heart Association Electrocardiography and Arrhythmias Committee CuoCC, Foundation ACoC and Society HR. Recommendations for the standardization and interpretation of the electrocardiogram. Part II: Electrocardiography diagnostic statement list. A scientific statement from the American Heart Association Electrocardiography and Arrhythmias Committee, Council on Clinical Cardiology; the American College of Cardiology Foundation; and the Heart Rhythm Society. *Heart Rhythm*. 2007;4:413-9.

83. Nadour W, Doyle M, Williams RB, Rayarao G, Grant SB, Thompson DV, Yamrozik JA and Biederman RW. Does the presence of Q waves on the EKG accurately predict prior myocardial infarction when compared to cardiac magnetic resonance using late gadolinium enhancement? A cross-population study of noninfarct vs infarct patients. *Heart Rhythm*. 2014;11:2018-26.

84. Loring Z, Chelliah S, Selvester RH, Wagner G and Strauss DG. A detailed guide for quantification of myocardial scar with the Selvester QRS score in the presence of electrocardiogram confounders. *J Electrocardiol*. 2011;44:544-54.

85. Anderson WD, Wagner NB, Lee KL, White RD, Yuschak J, Behar VS, Selvester RH, Ideker RE and Wagner GS. EVALUATION OF A QRS SCORING SYSTEM FOR ESTIMATING MYOCARDIAL INFARCT SIZE .6. IDENTIFICATION

OF SCREENING CRITERIA FOR NON-ACUTE MYOCARDIAL INFARCTS. *American Journal of Cardiology*. 1988;61:729-733.

86. Freye CJ, Wagner NB, Howe CM, Stack NC, Ideker RE, Selvester RH and Wagner GS. EVALUATION OF A QRS SCORING SYSTEM FOR ESTIMATING MYOCARDIAL INFARCT SIZE .8. SPECIFICITY IN A CONTROL-GROUP WITH LEFT-VENTRICULAR HYPERTROPHY AND PROPOSAL OF A NEW SCORING SYSTEM FOR USE WITH THIS CONFOUNDING FACTOR. *Journal of Electrocardiology*. 1992;25:19-23.

87. Hindman NB, Schocken DD, Widmann M, Anderson WD, White RD, Leggett S, Ideker RE, Hinohara T, Selvester RH and Wagner GS. EVALUATION OF A QRS SCORING SYSTEM FOR ESTIMATING MYOCARDIAL INFARCT SIZE .5. SPECIFICITY AND METHOD OF APPLICATION OF THE COMPLETE SYSTEM. *American Journal of Cardiology*. 1985;55:1485-1490.

88. Howe CM, Freye CJ, Wagner NB, Leggett SI, Behar JV, Jones MG, Hinohara T and Wagner GS. EVALUATION OF A QRS SCORING SYSTEM FOR ESTIMATING MYOCARDIAL INFARCT SIZE .7. SPECIFICITY IN A CONTROL-GROUP WITH RIGHT VENTRICULAR HYPERTROPHY DUE TO MITRAL-STENOSIS. *American Journal of Cardiology*. 1988;62:322-324.

89. Ideker RE, Wagner GS, Ruth WK, Alonso DR, Bishop SP, Bloor CM, Fallon JT, Gottlieb GJ, Hackel DB, Phillips HR, Reimer KA, Roark SF, Rogers WJ, Savage RM, White RD and Selvester RH. EVALUATION OF A QRS SCORING SYSTEM FOR ESTIMATING MYOCARDIAL INFARCT SIZE .2. CORRELATION WITH QUANTITATIVE ANATOMIC FINDINGS FOR ANTERIOR INFARCTS. *American Journal of Cardiology*. 1982;49:1604-1614.

90. Roark SF, Ideker RE, Wagner GS, Alonso DR, Bishop SP, Bloor CM, Bramlet DA, Edwards JE, Fallon JT, Gottlieb GJ, Hackel DB, Phillips HR, Reimer KA, Rogers WJ, Ruth WK, Savage RM, White RD and Selvester RH. EVALUATION OF A QRS SCORING SYSTEM FOR ESTIMATING MYOCARDIAL INFARCT SIZE .3. CORRELATION WITH QUANTITATIVE ANATOMIC FINDINGS FOR INFERIOR INFARCTS. *American Journal of Cardiology*. 1983;51:382-389.

91. Wagner GS, Freye CJ, Palmeri ST, Roark SF, Stack NC, Ideker RE, Harrell FE and Selvester RH. EVALUATION OF A QRS SCORING SYSTEM FOR ESTIMATING MYOCARDIAL INFARCT SIZE .1. SPECIFICITY AND OBSERVER AGREEMENT. *Circulation*. 1982;65:342-347.

92. Ward RM, White RD, Ideker RE, Hindman NB, Alonso DR, Bishop SP, Bloor CM, Fallon JT, Gottlieb GJ, Hackel DB, Hutchins GM, Phillips HR, Reimer KA, Roark SF, Rochlani SP, Rogers WJ, Ruth WK, Savage RM, Weiss JL, Selvester RH and Wagner GS. EVALUATION OF A QRS SCORING SYSTEM FOR ESTIMATING MYOCARDIAL INFARCT SIZE .4. CORRELATION WITH QUANTITATIVE

ANATOMIC FINDINGS FOR POSTEROLATERAL INFARCTS. *American Journal of Cardiology*. 1984;53:706-714.

93. Engblom H, Wagner GS, Setser RM, Selvester RH, Billgren T, Kasper JM, Maynard C, Pahlm O, Arheden H and White RD. Quantitative clinical assessment of chronic anterior myocardial infarction with delayed enhancement magnetic resonance imaging and QRS scoring. *Am Heart J*. 2003;146:359-66.

94. Horacek BM, Warren JW, Albano A, Palmeri MA, Rembert JC, Greenfield JC, Jr. and Wagner GS. Development of an automated Selvester Scoring System for estimating the size of myocardial infarction from the electrocardiogram *J Electrocardiol* United States; 2006(39): 162-8.

95. Bilchick KC, Kamath S, DiMarco JP and Stukenborg GJ. Bundle-branch block morphology and other predictors of outcome after cardiac resynchronization therapy in Medicare patients. *Circulation*. 2010;122:2022-30.

96. Chinitz JS, d'Avila A, Goldman M, Reddy V and Dukkipati S. Cardiac Resynchronization Therapy: Who Benefits? *Ann Glob Health*. 2014;80:61-68.

97. Chung ES, Leon AR, Tavazzi L, Sun JP, Nihoyannopoulos P, Merlino J, Abraham WT, Ghio S, Leclercq C, Bax JJ, Yu CM, Gorcsan J, 3rd, St John Sutton M, De Sutter J and Murillo J. Results of the Predictors of Response to CRT (PROSPECT) trial. *Circulation*. 2008;117:2608-16.

98. Zareba W, Klein H, Cygankiewicz I, Hall WJ, McNitt S, Brown M, Cannom D, Daubert JP, Eldar M, Gold MR, Goldberger JJ, Goldenberg I, Lichstein E, Pitschner H, Rashtian M, Solomon S, Viskin S, Wang P, Moss AJ and Investigators M-C. Effectiveness of Cardiac Resynchronization Therapy by QRS Morphology in the Multicenter Automatic Defibrillator Implantation Trial-Cardiac Resynchronization Therapy (MADIT-CRT). *Circulation*. 2011;123:1061-72.

99. Strauss DG, Selvester RH, Lima JA, Arheden H, Miller JM, Gerstenblith G, Marban E, Weiss RG, Tomaselli GF, Wagner GS and Wu KC. ECG quantification of myocardial scar in cardiomyopathy patients with or without conduction defects: correlation with cardiac magnetic resonance and arrhythmogenesis. *Circ Arrhythm Electrophysiol*. 2008;1:327-36.

100. Xia X, Wieslander B, Strauss DG, Wagner GS, Zareba W, Moss AJ and Couderc JP. Automatic QRS Selvester scoring system in patients with left bundle branch block. *Europace*. 2015.

101. Xia X, Chaudhry U, Wieslander B, Borgquist R, Wagner GS, Strauss DG, Platonov P, Ugander M and Couderc JP. Selvester scoring in patients with strict LBBB using the QUARESS software. *J Electrocardiol*. 2015.

102. (CDC) CfDCaP. Nephrogenic fibrosing dermopathy associated with exposure to gadolinium-containing contrast agents--St. Louis, Missouri, 2002-2006. *MMWR Morb Mortal Wkly Rep*. 2007;56:137-41.

103. Moss AJ, Brown MW, Cannom DS, Daubert JP, Estes M, Foster E, Greenberg HM, Hall WJ, Higgins SL, Klein H, Pfeffer M, Wilber D and Zareba W. Multicenter automatic defibrillator implantation trial-cardiac resynchronization therapy (MADIT-CRT): design and clinical protocol *Ann Noninvasive Electrocardiol* United States; 2005(10): 34-43.

104. Heiberg E, Ugander M, Engblom H, Götberg M, Olivecrona GK, Erlinge D and Arheden H. Automated quantification of myocardial infarction from MR images by accounting for partial volume effects: animal, phantom, and human study. *Radiology*. 2008;246:581-8.

105. Engblom H, Tufvesson J, Jablonowski R, Carlsson M, Aletras AH, Hoffmann P, Jacquier A, Kober F, Metzler B, Erlinge D, Atar D, Arheden H and Heiberg E. A new automatic algorithm for quantification of myocardial infarction imaged by late gadolinium enhancement cardiovascular magnetic resonance: experimental validation and comparison to expert delineations in multi-center, multi-vendor patient data. *J Cardiovasc Magn Reson*. 2016;18:27.

106. Cerqueira MD, Weissman NJ, Dilsizian V, Jacobs AK, Kaul S, Laskey WK, Pennell DJ, Rumberger JA, Ryan T, Verani MS and American Heart Association Writing Group on Myocardial Segmentation and Registration for Cardiac I. Standardized myocardial segmentation and nomenclature for tomographic imaging of the heart: a statement for healthcare professionals from the Cardiac Imaging Committee of the Council on Clinical Cardiology of the American Heart Association. *Circulation*. 2002;105:539-42.

107. Heiberg E, Sjögren J, Ugander M, Carlsson M, Engblom H and Arheden H. Design and validation of Segment--freely available software for cardiovascular image analysis. *BMC Med Imaging*. 2010;10:1.

108. Tufvesson J, Hedström E, Steding-Ehrenborg K, Carlsson M, Arheden H and Heiberg E. Validation and Development of a New Automatic Algorithm for Time-Resolved Segmentation of the Left Ventricle in Magnetic Resonance Imaging. *Biomed Res Int*. 2015;2015:970357.

109. DuBois D and EF D. A formula to estimate the approximate surface area if height and weight be known. *Arch Int Med*. 1916;17:863-71

110. Lang RM, Bierig M, Devereux RB, Flachskampf FA, Foster E, Pellikka PA, Picard MH, Roman MJ, Seward J, Shanewise JS, Solomon SD, Spencer KT, Sutton MS and Stewart WJ. Recommendations for chamber quantification: a report from the American Society of Echocardiography's Guidelines and Standards Committee and the Chamber Quantification Writing Group, developed in conjunction with the European Association of

Echocardiography, a branch of the European Society of Cardiology. *J Am Soc Echocardiogr*. 2005;18:1440-63.

111. Harrell FE, Jr., Lee KL and Mark DB. Multivariable prognostic models: issues in developing models, evaluating assumptions and adequacy, and measuring and reducing errors. *Stat Med*. 1996;15:361-87.

112. Dong YX, Powell BD, Asirvatham SJ, Friedman PA, Rea RF, Webster TL, Brooke KL, Hodge DO, Wiste HJ, Yang YZ, Hayes DL and Cha YM. Left ventricular lead position for cardiac resynchronization: a comprehensive cinegraphic, echocardiographic, clinical, and survival analysis. *Europace*. 2012.

113. Wieslander B and Atwater BD. The Selvester QRS score updated for use in conduction abnormalities: are we really ready to score? *J Electrocardiol*. 2015;48:69-70.

114. Strauss DG, Cardoso S, Lima JA, Rochitte CE and Wu KC. ECG scar quantification correlates with cardiac magnetic resonance scar size and prognostic factors in Chagas' disease. *Heart*. 2011;97:357-61.

115. Strauss DG, Poole JE, Wagner GS, Selvester RH, Miller JM, Anderson J, Johnson G, McNulty SE, Mark DB, Lee KL, Bardy GH and Wu KC. An ECG index of myocardial scar enhances prediction of defibrillator shocks: an analysis of the Sudden Cardiac Death in Heart Failure Trial. *Heart Rhythm*. 2011;8:38-45.

116. Wikstrom G, Blomström-Lundqvist C, Andren B, Lönnerholm S, Blomström P, Freemantle N, Remp T, Cleland JG and investigators C-Hs. The effects of aetiology on outcome in patients treated with cardiac resynchronization therapy in the CARE-HF trial. *Eur Heart J*. 2009;30:782-8.